

# University of Cincinnati

Date: 11/5/2013

I, Anna M Method, hereby submit this original work as part of the requirements for the degree of Master of Science in Molecular & Developmental Biology.

It is entitled:

**Development of cloacal organs in mouse and human**

Student's name: **Anna M Method**

This work and its defense approved by:

Committee chair: James Wells, Ph.D.

Committee member: Geraldine Guasch, Ph.D.

Committee member: Aaron Zorn, Ph.D.



6887

# Development of cloacal organs in mouse and human

A thesis submitted to  
the Graduate School of the  
University of Cincinnati  
in partial fulfillment of the  
requirements for the degree of

Master of Science

In the Department of Molecular and Developmental Biology of the College of Medicine

By

Anna M. Method

B.A. DePauw University, May 2007

November 2013

Committee Chair: James M. Wells, Ph.D.

## ABSTRACT

The cloaca is a transient embryonic structure that develops from the posterior hindgut that gives rise to the endodermal lining of the rectum, anus, and the urogenital system, including the bladder and urethra through a process known as septation. When this does not occur properly it can lead to anorectal and urogenital malformations, varying in severity from a simple fistula to complex anomalies like cloaca malformation. The developmental process of septation is poorly understood and the complex nature of these defects leaves much room for therapeutic treatment improvement. An overall lack of early cloacal markers makes identifying progenitor cells as well as following the identity of regions of the cloaca during development difficult. After identifying useful cloacal markers, K8 and Sox2, looking at the expression pattern during early development in mouse from e8.5 to e15.5, we mapped early cloacal domains that give rise to bladder, urethra, and parts of the anorectal system. We used these newly defined markers to establish a model of human cloaca development using a recently published method to derive gut tube structures (spheroids) from human embryonic stem cells. Given that the cloaca develops from the posterior hindgut, we hypothesized that posteriorizing factors could direct three dimensional spheroids into organoids containing cloacal progenitors that would form differentiated cells of the urogenital and anorectal tracts. Our data suggests that timing and dose of Wnt and BMP signaling posteriorized gut tube spheroids and that this promoted the subsequent formation of urothelial lineages. The ability to generate cloacal progenitors and its derivatives will allow study of anorectal and urogenital malformations in a human *in vitro* system, which could lead to new therapeutic treatments.



## Table of Contents

<b>Title Page</b>	<b>ii</b>
<b>Abstract</b>	<b>iii</b>
<b>Table of Contents</b>	<b>iv</b>
<b>Introduction</b>	<b>1-8</b>
<b>Materials &amp; Methods</b>	<b>9-14</b>
<b>Results</b>	<b>14-29</b>
<i>Novel Expression domains of Sox2, Cytokeratin 8 and FoxA2 mark early regional domains of the hindgut and cloaca</i>	<b>14-17</b>
<i>Shh knockout animals lose K8 and Sox2 expression</i>	<b>17-18</b>
<i>Active BMP signaling in early developing cloaca</i>	<b>18-19</b>
<i>Using human PSCs to model cloaca development</i>	<b>19-25</b>
<i>Temporal effects of Chiron/FGF4 to further posteriorize tissue</i>	<b>25-26</b>
<i>Investigating the synergistic effects of Chiron/FGF4 and both BMP timing and concentration to posteriorize tissue</i>	<b>26-29</b>
<b>Discussion</b>	<b>29-36</b>
<b>Figures &amp; Tables</b>	<b>37-55</b>
<b>Supplemental Figures</b>	<b>56-68</b>
<b>References</b>	<b>69-72</b>

## INTRODUCTION

### *The Cloaca*

The most posterior portion of the hindgut gives rise to a transient embryonic structure in mammals known as the cloaca. The cloaca is defined at e10.5 in the mouse embryo as a small cavity at the posterior end of the gut tube. This cavity is a transient structure lined with endoderm and surrounded by mesenchyme that when patterned properly gets subdivided into regions that give rise to the endodermal lining of the rectum, anus, and the urogenital system, including the bladder, urethra, and prostate in males (Seifert 2008, Cunha 2004). Formation of these organ lineages involves a morphogenetic process known as septation. The process of septation begins shortly after the cloacal cavity forms at e10.5, with the formation of the urorectal septum. The urorectal septum is composed of mesenchyme and it is believed that the septum pushes forward such that after 3 days there is complete separation of the cloacal cavity into separate openings for the digestive and urogenital tracts. This process is complete by e13.5 in the mouse embryo. Interestingly, the process of septation has been a topic of debate for many years.

### *Stages of cloaca development: Cloaca formation and patterning*

Though much is known about anterior-posterior and dorsal-ventral patterning of the gut tube that gives rise to the intestinal tract, far less is understood about cloaca specification, patterning, and septation. In fact, almost nothing is known about what specifies the portion of the hindgut that becomes the cloaca. Mouse models of anorectal and urogenital malformations have a cloaca, suggesting that these genes are not involved in the actual specification of cloacal cells. For instance, *Shh* null embryos have

complete loss of Shh signaling from the beginning of development, yet they develop an embryonic cloaca which persists later as a cloaca malformation, suggesting Shh is not necessary for cloacal specification (Mo 2001). The same is true for BMP7 null animals (Wu 2009). Both Shh and BMP7 are studied due to malformations of the cloaca, but these observed defects are not due to lack of specification of hindgut tissue, rather are the result of improper septation. In addition to little being known about what specifies the caudal hindgut to become the cloacal cavity, how the tissue is patterned is also unknown. One study suggested that the dorso-ventral patterning of the cloaca may involve Wnt5a. Analysis of human embryos showed expression of Wnt5a predominately on the dorsal side of the cloaca that becomes anus and rectum. The ventral side, which gives rise to the urogenital sinus, almost entirely lacked expression (Li 2011). This suggests that Wnt5a may play a role in early patterning that specifies portions of the cloaca to become part of the anorectal system versus the urogenital system.

#### *Stages of cloaca development: Cloaca septation*

Most work on understanding the cloaca revolves around the process of septation. Work using a tamoxifen inducible Shh CreER to remove Shh signaling from the endoderm at different developmental time points has shown Shh has both early and late functions during the process of anorectal and urogenital development. When Shh signaling is lost early, around e9.5, the intestine is very short and meets the cloaca in a much more anterior position due to septation failure. At slightly later stages of cloaca development (e10.5-e13), Shh regulates the process of septation as well as genital tubercle outgrowth. The degree of septation observed is directly related to the length of

active Shh signaling. Therefore, the longer Shh was active in embryos the further septation is able to progress. Progression of septation correlates to the position at which the gut meets the cloaca, thus the longer Shh is active the further septation has advanced, and the more posterior the connection of the gut tube to the cloaca. It is believed that Shh signaling from the endoderm regulates the process of septation through increased cell proliferation of the posterior urorectal septum mesenchyme (Seifert 2009). Shh null mice do show some septation suggesting other pathways are at work, or compensate for the loss of Shh signaling.

More recently studies in mice focus on the molecular mechanisms and other signaling pathways that could support models of cloacal septation. Most work suggests that septation is the result of the morphogenetic movements of the urorectal septum as the result of proliferation. In support of that, studies using BMP7 null mice show that the urorectal septum moves forward through cellular morphogenetic movements promoted by BMP7 signaling from the mesenchyme, which induces cloacal endoderm cell survival, as well as proliferation of the endoderm and surrounding mesoderm (Wu 2009). Further study identified that BMP7 also acts to promote proper polarity of cells during division, and that promotion of the apical basal orientation of cell division leads to the separation of the cloaca into separate urogenital and intestinal tracts (Xu 2012). This finding yields a mechanism and understanding of how septation occurs and how the urorectal septum pushes forward by proper polarity of cell division. Wnt5a, a noncanonical Wnt ligand, also has been shown to be critical for proper septation, as knockouts have imperforate anus and shortened intestinal tracts, which is believed to be in part due to their defects in cell proliferation (Tai 2009). Interestingly, Wnt5a has been

shown to act through the JNK pathway in other contexts, and be involved in cell polarity, which coordinates with the BMP7 data that suggests the apical basal cell division is regulated through JNK (Gros 2010, Xu 2012).

Lastly, two transcription factors, Six1 and Six2, have been shown to be asymmetrically expressed in the peri-cloacal mesenchymal progenitors and that they are required for proper development of the anorectal (anorectal-urogenital) system. It is hypothesized that this asymmetrical expression leads to unbalanced growth of the mesenchyme. The asymmetrical growth is believed to be the driving force that septates the cloaca (Wang C. 2013). Loss of these transcription factors, or their co-activator Eya1, leads to a significant decrease in peri-cloacal mesenchyme cell survival and proliferation (Wang C 2013, Wang C 2011). Interestingly, these transcription factors influence both BMP4 and BMP7 levels, such that loss of Six factors results in BMP up-regulation. In addition the loss of Six factors also up-regulated Dkk1 and Dkk2, which are inhibitors of the Wnt pathway and a downstream effector for BMP signaling (Wang C 2013). All in all, correct expression of Six factors is required for proper development of the anorectal and urogenital system, likely due to their ability to disrupt very important signaling pathways required for development. It is possible that these signaling pathways and transcription factors are all acting together for proper septation; however this has yet to be defined.

#### *Cloaca development and malformations in humans*

As mentioned above, the process of septation is a relatively quick developmental process, completing in three short days in the mouse embryo and by the sixth

gestational week in humans (Warne 2010). There are multiple theories on how the cloaca becomes divided during development, though the exact mechanism that drives septation and cloacal development are unclear. Work done in mammals in the late 1880s by Tourneux and Retterer resulted in the acceptance that the cloaca became subdivided by the movement of the urorectal septum; however they had differing views on the nature of the movement. Tourneux believe the septum would shift from cranial to caudal “like a French Curtain”, whereas Retterer believed there were lateral ridges that would form on either side of the cloaca and that these would begin fusing at the cranial end and continue downward until fusion at the caudal cloaca completed. Over the next 6 decades this was the standard belief, until the mid 1950s, when several groups began studying anorectal malformations in newborns and concluded that the rectum “migrates” during normal development. This theory however, was never shown by any piece of scientific evidence, rather was a hypothesis based on imperforate anus defects. But shortly thereafter van der Putte suggested a modified theory of “rectal migration”, in which he believed there was a shift of the dorsal cloaca, moving towards the rear in order to establish the anal opening (reviewed in Kluth 2010). The theory of lateral fold fusion and rectal migration were dismissed in 1995 after work done in rat embryos found no evidence of these mechanisms of cloacal division. Current studies hope to identify the mechanism of cloacal septation that promotes movement of the urorectal septum to divide the cloacal cavity.

Defects in the septation and development process lead to clinically significant anorectal and urogenital malformations, including imperforate anus, hypospadias, various fistulas, and most severely, cloaca. Some anorectal malformations are

associated with various syndromes such as VACTERL, trisomies, or Currarino syndrome and occasionally have associated spinal anomalies of the sacrum. Other malformations are non-syndromic and are not associated with other defects (Levitt 2007). The malformation cloaca is a defect observed in females, sometimes referred to as persistent cloaca (Warne 2011). It is characterized by the lack of division between the rectum, urethra, and vagina, resulting in what is known as a common channel. The length of this common channel varies and often determines the prognosis for bowel and urinary control (Levitt 2010). In correlation with animal studies, a link between patients with anorectal malformations and gene expression levels of BMP4 and Shh has been identified. This study shows that there is a correlation between the type of defect, “high” or “low” anorectal malformations, and expression. Patients with “low” malformations only showed decreased levels of GLI2, a transcription factor that is regulated by Shh, while patients with “high” malformations showed down-regulation of both Shh and BMP4 (Zhang 2009). In addition to patient cases involving BMP and Shh signaling, rare cases of human genetic disorders like hand-foot-genital syndrome have been linked to specific genes, in this case there is a mutation in the HoxA13 locus (Mortlock 1997). Though some malformations have been shown to involve these signaling pathways many malformations remain of unknown cause.

### *The use of hESC to model human disease*

Studies utilizing human embryonic stem cells have become more common in recent years and many have shown that induced pluripotent stem cells (iPSCs) can be used to study human disease. For instance, human iPSC lines have been used to

model congenital cardiac arrhythmias *in vitro*, allowing for individual patient disease modeling and hopes of individualized therapeutic drug testing (Itzhaki 2011). Moreover, hESC and iPSC derived cell types are being used therapeutically to alleviate symptoms in disease models of diabetes and multiple sclerosis. For example iPSC derived oligodendrocytes rescue a mouse model of congenital hypomyelination, and pancreatic endoderm generated from hESCs, implanted into mice produce glucose responsive endocrine cells that exhibit properties of functional beta-cells (Wang S. 2013, Kroon 2008).

The ability to utilize hESCs and iPSCs as a tool to study disease and malformation is vital to better understanding diseases in a human genetic background, especially for conditions where there is not a useful disease model that relates to human conditions, cases where human samples are difficult to obtain, or when studies require embryonic tissue. Thus for the study of cloaca malformation in humans, hESCs and iPSCs hold great value as human embryonic tissue samples are difficult to obtain and animal models often focus on only certain aspects of malformation, such as specific gene knockout. The ability to study defects within a diseased patient's cells, via iPSCs would give a much greater depth of understanding, allowing for global study of not only gene defects, but effects on signaling pathways. Before studying defects in patient samples via iPSCs, the ability to reproducibly generate cloacal tissue in hESCs is necessary.

### *Generating posterior gut tube from hESC cultures*

As described earlier, the cloaca is an endoderm lined cavity at the posterior end of the gut tube. Thus to direct the differentiation of hESCs into a cloacal like fate would require the endoderm to be patterned distally to generate the most posterior hindgut possible. Studies suggest that several signaling pathways are important for the anterior-posterior patterning of endoderm. FGF signaling is known to be a vital signaling factor in the establishment of the A-P axis of the gut tube by promoting posterior fate and repression of Wnt signaling is needed to establish anterior and midgut organ development, suggesting Wnt signaling is needed for posteriorization (Dessimoz 2006, Wells 2000, McLin 2007). Protocols to efficiently generate definitive endoderm (DE) from hESCs, as well as three dimensional cultures of intestinal tissues *in vitro* lay the foundation for patterning hESCs into a cloacal-like tissue (D'Amour 2005, Spence 2011, McCracken 2011).

### *Posteriorizing pathways as candidates for cloacal inducers*

As discussed above, the cloaca derives from the posterior region of the hindgut. Therefore, in order to generate a cloaca-like tissue, we hypothesize that increased activation of posteriorizing pathways would be required. In addition to FGF and WNT, BMP has been demonstrated to have posteriorizing activity in frogs, fish, and chick (Rankin 2011, Tucker 2008, Kumar 2003). Moreover, the levels of these signaling pathways can be easily modulated by the dose and/or duration of signaling activation in culture. We hypothesize that three dimensional mid/hindgut spheroids can be patterned

into cloacal-like tissue by increasing the signaling levels of posteriorizing pathways, specifically WNT and BMP signaling, at early stages of spheroid generation.

## **Materials and Methods**

### *Mouse embryo collection and processing for paraffin*

CD1 wild-type mice purchased from Jackson Laboratories were mated and the day a vaginal plug was visible was considered 0.5 embryonic days. Embryos were collected by dissection with surgical tools and placed in 4% paraformaldehyde (PFA) overnight at 4°C. The following day, embryos are washed 3 times in 1x PBS for 30 minutes each, followed by dehydration in a graded series of ethanol rinses (30%, 50%, 75%, 85%, 90%, 95%, 100%) for 30 minutes each. Preparation for paraffin embedding was followed with 30 minutes in a 1:1 ratio of 100% ethanol to xylene, 100% xylene for 15-30 minutes (dependent on embryo size), xylene to paraffin 1:1 for 30 minutes, and then 3 consecutive 1 hour paraffin rinses. After processing embryos are left at room temperature in paraffin overnight prior to embedding. The day of embedding, embryos are placed into hot paraffin bath to melt. Embryos are oriented sagittally in plastic molds and cooled overnight. Tissue is serial sectioned on placed on glass slides at 7 microns thick.

### *Immunohistochemistry*

Sectioned embryos were deparaffinized following standard procedures consisting of 3 xylene washes, and an ethanol to H<sub>2</sub>O graded rehydration series (100%-30%), a 5 minute rinse in water, followed by antigen retrieval. Antigen retrieval was conducted in

sodium citrate buffer solution in a steamer for 30 minutes. Blocking was completed following the protocol outlined in the Mouse on Mouse (M.O.M) Basic Kit by Vector Laboratories when mouse antibodies were used; otherwise 10% normal donkey serum (NDS) in PBS-T was used for blocking. Primary antibodies were applied in MOM Diluent solution overnight at 4°C for mouse primaries, or 5% NDS in PBS-T. Primary antibodies included: Sox2 (Rabbit, Seven Hills Bioreagents, Cincinnati, OH 1:2000), Cdx2 (Mouse, Biogenex, Fremont, CA, 1:300), FoxA2 (Goat, Santa-Cruz, 1:250), Pdx1 (Goat, AbCam, 1:5000), Upk1a (Goat, Santa-Cruz, 1:300). Secondaries were incubated at room temperature for 45 minutes in MOM Diluent at 1:500, or in 5% NDS in PBS-T. Secondaries included: Donkey anti-goat Alexa Fluor 488, Donkey anti-rabbit Cy3, Donkey anti-mouse Dylight 649, (Jackson ImmunoResearch Laboratories, Inc. West Grove, PA). DAPI was used as a nuclear stain. All slides were cover-slipped using Fluoromount-G (Southern Biotechnology Associates, Inc., Birmingham, AL). Staining of stem cell monolayers as well as cryo-sections of organoids is carried out using a blocking buffer of 10% normal donkey serum (NDS) in 0.05% PBS-T. Primary antibodies are diluted in 5% NDS in PBS-T, as are secondaires. Incubation times and dilutions are the same.

#### *Whole mount immunostaining*

Both CD1 wild-type embryos and B6.Cg-*Shh*<sup>tm1(EGFP/cre)Cjt</sup>/J in a C57Bl6 background were purchased from The Jackson Laboratory (Bar Harbor, Maine, USA). Embryos were harvested at specific stages and stages e10.5 and above had excess tissue removed (ie. Limb buds and/or ectoderm/mesoderm surrounding genital tubercle)

to allow for proper antibody penetration. After dissection embryos were fixed in 4% paraformaldehyde overnight at 4°C. Embryos were washed briefly in 1x PBS and transferred to 100% methanol before placing in -20°C for a minimum of 24 hours. Upon starting the staining process embryos are placed in “Dent’s Bleach”, a solution of methanol, DMSO, and hydrogen peroxide at a ratio of 4:1:1 respectively for 2 hours. Embryos are then rehydrated in a graded series of methanol rinses (100%, 75%, 50%, and 25%) before being placed in 0.5% TSA block (Invitrogen TSA kit T20922 component D) diluted in 0.5% Triton-X for 3 hours. Primary antibodies are diluted in TSA blocking reagent and incubated overnight at 4°C. Primary antibodies were used at the following dilutions: Keratin 8 (Rat, Developmental Hybridoma Bank 1:10), Sox2 (Rabbit, AbCam, Cambridge, MA, 1:2000), FoxA2 (Goat, Santa-Cruz Biotechnology Inc., Santa Cruz, CA, 1:250), pSMAD1,5,8 (Rabbit, Cell Signaling, Beverly, MA 1:800). Following overnight incubation embryos were washed in five 1 hour rinses in 0.5% PBS-T. Secondary antibodies were diluted in TSA blocking reagent and incubated overnight at 4°C. Secondaries included: Donkey anti-rat Alexa Fluor 488, Donkey anti-rabbit Cy3, Donkey anti-goat Dylight 649, (Jackson ImmunoResearch Laboratories, Inc. West Grove, PA) at a dilution of 1:500. Embryos were again washed in 0.5% PBS-T for three 1 hour washes before being placed in 100% methanol. Prior to imaging embryos are cleared in “Murray’s Clear”, a solution consisting of benzyl alcohol and benzyl benzoate at a ratio of 1:2 respectively for 30 minutes prior to imaging. Immunostained embryos are imaged using a Nikon A1R-Si laser scanning confocal on a Nikon Eclipse Ti inverted microscope. Processing of images for 3 dimensional whole mount stacks and slices were made using Imaris 7.6.4 software.

### *Quantitative Real-Time PCR of spheroids and organoids*

Spheroid samples were collected at day of harvest, where approximately 75-100 spheroids were pooled into an eppendorf tube, and stored at -80°C until RNA extraction. Organoids were collected by careful removal of matrigel using microdissection tools at both 28 and 56 days. Organoids were isolated 3 per condition for biological triplicate analysis when available. Samples were stored at -80°C prior to RNA isolation. Total RNA was extracted using the RNeasy Micro Kit (Qiagen) according to manufacturer instructions. Concentration of RNA samples was measured using a NanoDrop 2000 (Thermo Scientific) and approximately equal amounts of RNA for each sample were then reverse transcribed into cDNA using the SuperScript III First-Strand Synthesis System (Invitrogen). Real-time PCR was performed using QuantiTect SYBR Green (Qiagen) on a BioRad CFX96. Primers used can be found in Table 1. All analysis was completed using Microsoft Excel. All samples were normalized for relative expression compared to EGF control samples as indicated. Student t-tests (1 tail, unpaired) were completed to determine statistical significance when adequate sample number was available. Table 3 shows trends of gene expression increase over EGF controls by quantifying the number of BMP treated organoids that have 3 fold or higher increases in relative gene expression over controls. Table 4 combines all experiments done in biological triplicate and looks at the number of experiments where increases in gene expression were statistically significant over EGF controls.

### *hESC Culturing*

Low passage WA01-feeder free (H1) human embryonic stem cells were obtained from the Pluripotent Stem Cell Facility at Cincinnati Children's Hospital. Cells were maintained by regular passaging via dispase splitting at a ratio of 1:6 wells of a 6 well plate coated with hESC-qualified matrigel matrix (BD Biosciences). Cells are maintained with daily changes of mTSER media (Stem Cell Technologies). For differentiation into definitive endoderm we utilized a previously published protocol by D'Amour (D'Amour 2005). Cells are dispase split at a ratio of 4 wells of a 6 well into a 24 well plate and maintained in mTSER until the colonies are 60-70% confluent, approximately 2 days after plating. Activin A (R&D Systems) is used at 100ng/mL for three days in RPMI 1640 media (Invitrogen) with increasing concentrations daily (0%, 0.2%, 2%) of HyClone defined FBS (Thermo Scientific). Following 3 days of Activin A differentiation into DE, cells were treated with 500ng/ml FGF4 (R&D Systems) and 3uM Chiron (CHIR99021, Stemgent) in 2% dFBS-DMEM/F12 for 4 days. Three dimensional floating spheroids begin budding off, differentiation dependant, starting on day 3 or day 4 of Chiron/FGF4 treatment. If Chiron/FGF4 is continuously applied, spheroids can bud off the monolayer up to day 8 of treatment.

### *Spheroid Plating and Maintenance*

The day of spheroid isolation is considered day 0. Spheroids are collected and pooled into eppendorf tubes and allowed to settle, then after careful removal of excess media, all spheroids are pooled into one tube. Approximately 500 spheroids are mixed into a 500uL aliquot of matrigel matrix (BD Biosciences) such that when 50uL matrigel

bubbles are plated there are approximately 50 spheroids per well. Plates are incubated for 15 minutes prior to the addition of organoid growth media. Growth media contains advanced DMEM-F12 (Invitrogen), B27 supplement (Invitrogen), N2 Supplement (R&D Systems), L-glutamine (Invitrogen), penicillin-streptomycin(Invitrogen), HEPES buffer (Invitrogen), and EGF (R&D Systems) (Adapted from McCracken 2011). For treatment conditions other than control media (EGF), BMP2, BMP4, or BMP7 (R&D Systems) can be added at appropriate concentrations (Standard for experiments is 100ng/mL unless otherwise stated). Media is changed every 4 days. Spheroids are allowed to grow in matrigel bubbles for 14 days before splitting and re-plating is required due to matrigel breakdown. As spheroids grow out into organoids, maintenance splitting every 14 days is done, and organoids can be cut using a scalpel. To re-plate, organoids are carefully removed from matrigel using dissection tools in warm advanced DMEM, and then placed in fresh matrigel matrix. After initial treatments with BMP all organoids are maintained in organoid growth media.

### *Organoid Collection and Processing*

Organoids are collected by careful removal of matrigel matrix using dissection tools and placed in cold 4% PFA for 1-2 hours dependent on size. Organoids are then washed in PBS, 3 washes over 3 hours, and placed in 30% sucrose (in PBS) overnight. The following day organoids are placed in a plastic mold and covered with Tissue-Tek O.C.T. compound, allowed to equilibrate for 30 minutes, and frozen on a dry ice-ethanol bath prior to storage in -80°C freezer. Samples are serial sectioned at a thickness of 8 microns using a cryostat and stored at -80°C until stained.

## RESULTS

### *Novel Expression domains of Sox2, Cytokeratin 8 and FoxA2 mark early regional domains of the hindgut and cloaca*

The patterning of the early cloaca into presumptive organ domains has not been studied, largely due to the absence of defined molecular markers. We analyzed the expression pattern of several genes in the developing cloaca and identified a pattern of expression that marks distinct domains in the developing cloaca as early as e9. The most useful markers include: *Foxa2*, which is broadly expressed in endoderm; *Cdx2*, which marks the intestine; Cytokeratin 8 (K8), known to be expressed in simple-type epithelium and strongly lines the urogenital sinus (UGS) or presumptive bladder; *Sox2*, which is expressed the dorsal region of the cloaca that gives rise to the anal canal and ventrally the urethra. While lineage tracing would be needed to definitively state that these early expression domains give rise to later cloacal derived organs, these markers have proven useful to monitor regionalization and development of cloacal derivatives.

The expression of *Cdx2* begins in a proximal location of the gut tube, the duodenum, where it is co-expressed with factors like *Pdx1*, and then continues to be expressed independently of *Pdx1* throughout the more posterior regions such as the intestines and colon. At early stages *Cdx2* is found throughout the hindgut endoderm and *Sox2* is found in foregut endoderm. Whole-mount immunohistochemistry on mouse embryos looking at the expression pattern of *Sox2* during cloaca development resulted in identification of a small population of distal endoderm cells expressing *Sox2*, starting around e8.5 in the mouse embryo (Figures 1, 2, Supplemental Figure 1). The *Sox2* expression identified co-expresses with the endoderm marker *FoxA2* in the posterior

hindgut and tail gut. Interestingly, these Sox2 cells are restricted to the most dorsal side of the gut tube during the early stages of development, at both e8.5 and e10.5 (Figure 1, Figure 2A), but expression at e11.5 shows expansion of these Sox2 cells into the ventral regions of the cloacal endoderm (Figure 2B, B'). What's more, these cells are also co-expressing Cdx2 at e10.5 (Figure 1C,D), an expression profile not reported previously during normal mouse development. Due to issues with mouse on mouse immune-detection other stages of expression were difficult to interpret, but results indicated Cdx2 may not continue its co-expression with Sox2 past e10.5 (Figure 3, Supplemental Figure 2). We hypothesize the co-expression of Sox2 and Cdx2 may resolve prior to e11.5 as a result of patterning and specification. We did not observe continued Cdx2 expression at later stages in the developing anal canal, consistent with expression data from the literature showing Cdx2 is not expressed distal intestine after e13.5, but is isolated to more proximal intestinal regions (Figure 3, Silberg 2000). Although, we have observed significant Cdx2 antibody variability, our inability to detect Cdx2 in the distal hindgut at earlier stages might be due sub-optimal Cdx2 antibody sensitivity. We believe that this early population of Sox2 expressing cells identified at e8.5 mark the dorsal cloaca progenitor cells that will give rise to the cells lining the dorsal cloacal, which later become the anal canal.

Restriction of cloacal markers occurs early and is continued throughout development. K8 appears to be regionally restricted by e10.5 to the ventral anterior domain of the cloaca that likely gives rise to the urogenital sinus (Figure 2 A, A', A"). Though we have not confirmed this through lineage tracing, we believe that this domain of K8 expression at e10.5 is already marking the region that is specified to become

urogenital sinus, and ultimately bladder. As development continues, the intense K8 expression expands within the developing urogenital sinus, as the dorsal Sox2 expression expands ventrally, lining not only the dorsal gut tube and regressing tail gut, but also and the ventral portion of the cloaca (Figure 2 B, B', B"). By e12.5 the K8 expression intensifies in the urogenital sinus as well as the developing ureters, and the Sox2 expression is now restricted to the anal canal that is being portioned off by the process of septation, as well as the remaining cloacal cavity that is beginning to elongate into the presumptive urethra (Figure 2 C, C', C"). As septation completes at e13.5 the expression of these markers is still compartmentalized (Figure 2 D, D', D"). Though the expression of these markers is not necessarily unique in the embryo, this defined pattern of expression observed in wild-type mouse embryos is reproducible, with only subtle variation, suggesting this pattern of marker expression could be extremely useful in analyzing early cloacal defects in mouse models and for directing differentiation of hESCs into cloacal derivatives.

#### *Shh knockout animals lose K8 and Sox2 expression*

It is well known that Shh is required for proper septation of the cloaca during mouse development and that it is expressed throughout the cloacal endoderm (Mo 2001, Seifert 2009). However, the role for Shh signaling at earlier stages of cloacal patterning has not been investigated. In collaboration with Laura Runck and Dr. Geraldine Guasch we used our newly defined early cloacal markers and whole mount immunofluorescence to investigate if Shh embryos exhibit early cloacal patterning defects. We first confirmed previous findings that Shh null embryos have improper

cloacal septation, improper genital tubercle growth, and often results in lack of external genitalia and a common opening for the urogenital and anorectal tracts (Mo 2001). We then analyzed the cloacal patterning of these knockout animals at e11.5, a time point in development that is prior to septation. Using whole-mount immunostaining and three dimensional imaging, we observed that the cloaca is smaller and malformed compared to wild-type controls as expected based on published reports, but also showed dramatic changes in the expression of K8 and Sox2. In KO embryos there is a significant reduction of Sox2 levels in the cloacal endoderm as compared to wild-type littermates (Figure 4). In addition, the strong expression of K8 was dramatically reduced or lost in Shh KO embryos (Figure 4, Runck 2013). The perturbation of regional markers K8 and Sox2 in Shh KO embryos suggests that early cloacal patterning is disrupted and is the underlying cause of later septation defects and urogenital malformations. These data identify the importance of early development and patterning of the cloaca, a poorly understood process.

#### *Active BMP signaling in early developing cloaca*

The cloaca derives from the posterior hindgut, which is the most posterior endoderm derivative. BMP signaling has long been known to play a role in posterior patterning of endoderm and mesoderm (Kumar 2003). However, little is known about the role of BMP signaling in patterning the posterior hindgut which gives rise to the cloaca. Studies in zebrafish show that BMP signaling is needed for proper function of the fish cloaca (Pyati 2006). In order to assess the possibility of BMP signaling having a role in cloacal endoderm specification and patterning we assessed regions of active

BMP signaling at early stages in hindgut and cloaca development by analyzing for phosphorylated SMAD1,5,8 proteins. These are downstream effectors of BMP signaling and become phosphorylated in response to BMP signal. Analysis of active BMP signaling by whole-mount immunohistochemistry identified active BMP signaling domains in e8.5 and e9.5 mouse embryos. At e8.5 strong pSMAD1,5,8 staining is observed throughout the embryo with the strongest staining observed along the length of the dorsal neural tube as previously reported (Eom 2011), and intensity increasing in the entire posterior tail region (Figure 5A). Closer examination of the posterior tail through optical slices shows strong nuclear staining in the posterior mesenchyme and endodermal lining of the gut tube (Figure 5A', 5A''). At e9.5 embryos had strong staining in the tail mesenchyme surrounding the gut tube, as well as weaker, though positive staining within the gut tube wall (Figure 5B, 5B', 5B''). Taken together, these data indicate that there is a gradient of active BMP signaling in the developing hindgut with the highest levels of pSMAD1,5,8 in the most posterior as well as ventral regions of the gut and mesenchyme (Figure 5C). The observation of strong pSMAD1,5,8 staining in the posterior regions of the hindgut at these early stages suggest BMP signaling could play a role in cloaca specification, and the dorsal-ventral gradient could play a role in cloacal patterning.

#### *Using human PSCs to model cloaca development*

Studying cloaca development and malformations in children has largely relied on samples from aborted fetuses, pig and sheep embryos, work in rats using chemically induced malformations, or mouse models with specific gene knockouts such as Shh/Gli

(Penington 2002, Jia 2011, Kimmel 2000). Unfortunately many anorectal and urogenital malformations are the result of cloacal defects and are of unknown cause, or multifactorial. In addition, cloacal development varies from species to species making comparisons difficult (Penington 2002). Particularly for studying defects in humans, lack of samples and difficulty obtaining samples makes exploring these congenital malformations difficult. With recent technological advances in creating induced pluripotent stem cells from patients with various deficiencies we believe that studying development in a human *in vitro* system would provide a powerful model to study early cloacal development (Beltrao-Braga 2013). Moreover we hypothesize that we can use known endoderm and hindgut posteriorizing pathways to generate three dimensional posterior hindgut and cloaca-like organoids in much the same way as recently generated intestinal organoids (Spence 2011, McCracken 2011). In this approach, human embryonic stem cells were first differentiated into definitive endoderm (DE) with Activin A (D'Amour 2005). The DE is produced by treating hESCs with ActivinA to yield a flat sheet of cells, similar to the e7.5 mouse embryo, which can be patterned into a hindgut fate through the addition of Wnt and FGF4 (Figure 6) (Spence 2011). In our studies we used Chiron rather than Wnt, a GSK-3 inhibitor. By inhibiting GSK-3 in the Wnt pathway, we are effectively keeping Wnt signaling active, by removal of a key component of the destruction complex that stops Wnt signaling. The combined effects of active Wnt signaling and FGF4 lead to the production of three dimensional budding spheroids off the DE monolayer. These spheroids are expressing Cdx2 and are reminiscent of an early e8.5 mouse embryos mid and hindgut endoderm gut tube (Figure 6). Spheroids can be embedded in matrigel, a matrix supporting three

dimensional growth, and cultured to give rise to tissue that expresses intestinal markers (Figure 6, Spence 2011).

The cloaca derives from the posterior hindgut. We therefore hypothesized that treatment of hindgut spheroids with posteriorizing factors such as BMP would direct spheroids into a cloacal fate, which we would be able to identify using the markers we defined to analyze early cloaca development in mouse embryos (Figure 6, Figure 2). Using a protocol very similar to that for generation of intestinal tissue, we generated spheroids harvested off of a Chiron/FGF4 monolayer after three days of treatment. Spheroids were embedded in matrigel and treated with BMP2 at 100ng/mL for three days in attempts to direct a posterior/cloacal fate, or EGF as a control. At 28 days organoids were analyzed by qPCR as well as immunohistochemistry. As hypothesized, posteriorization through the treatment of hindgut spheroid tissue with BMP2 resulted in what appeared to be a cloacal tissue. The epithelium of the organoid was expressing Cdx2 that was completely separate from intense Sox2 staining, all of which expressed K8 (Figure 7A). The control organoid, treated only with EGF, had an epithelium expressing both Cdx2 and K8, but was completely negative for Sox2 (Figure 7B). Interestingly the BMP2 treated organoid was very reminiscent of an e12.5 mouse embryo, with Sox2 expression in the anal canal and urethra being completely separate from the Cdx2 expression observed in the intestine (Figure 7D). Analysis of organoids by qPCR indicate that the BMP2 organoids showed increased levels of the posterior markers HoxA13 and HoxD13 as compared to the EGF control organoids. Though the control organoids and BMP2 treated organoids had similar expression levels of Cdx2,

the level of Sox2 was significantly increased in BMP2 treated samples, confirming the observed intense Sox2 staining seen in Figure 7A (Figure 7C).

We next used this approach to determine which BMP ligands may be involved in patterning and formation of cloacal-like tissues. The literature supports a role for BMP4 and BMP7 in posterior embryonic patterning and for later cloacal septation (Wu 2009, Sasaki 2004, Xu 2012 ). Thus we hypothesized that these other BMP ligands, specifically BMP4 or BMP7 may be better able to generate cloacal tissue and its derivatives. We therefore treated Chiron/FGF4 generated spheroids for three days with BMP2, 4 or 7 and monitored for the development of cloacal markers. There were significant differences observed in organoid morphology between BMP2, 4, 7 organoids at both 28 and 56 days of culture (Supplemental Figure 10A). Marker analysis suggests that BMP4 treatment yielded organoids that contained few Sox2 positive cells in the epithelium, but was able to induce expression of Cdx2 and both HoxA13 and HoxD13 levels above control EGF organoids as measured by qPCR (Figure 8, Tables 3 & 4). The levels of Cdx2 expression were comparable to BMP2 treated organoids (BMP2 data is the same in Figures 7 and 8). Though BMP4 organoids had higher levels of Hox genes than EGF, the levels were far below that of BMP2 organoids, suggesting that BMP2 is far superior at posteriorizing three day spheroids than BMP4. Interestingly BMP7 showed no ability to posteriorize spheroids. In fact, BMP7 organoids had lower levels of Cdx2 than controls, suggesting that BMP7 does not have posteriorizing activity and does not generate cloacal-like tissues (Figure 8, Tables 3 & 4).

All organoids had broad regions of epithelium expressing Cdx2. Since Cdx2 is a marker of all intestinal epithelium, including regions of the small and large intestine, it

was not clear what type of intestinal epithelium was being produced by BMP2, 4 or 7. We went on to look for other markers to better identify the regional identity of Cdx2 expressing epithelium seen in the different conditions. One marker of proximal intestine is Pdx1, which is co-expressed with Cdx2 in the duodenum. Analysis of EGF derived organoids showed that much of the epithelium was Cdx2/Pdx1 double positive indicating a duodenal fate. In contrast, BMP2 treated organoid showed no Pdx1 staining, suggesting that the Cdx2 positive cells were more distal intestine (Figure 9B, B'''). The distal nature of BMP2 organoids was confirmed by expression of HoxA and D13 (Figure 8). Interestingly, EGF, BMP4, and BMP7 cultures expressed lower levels of HoxA13 and HoxD13 and these organoids were broadly Pdx1/Cdx2 double positive suggesting that they were more proximal intestine (Figure 8, 9A', C', D'). Consistent with this, EGF, BMP4, and BMP7 organoids were Sox2 negative (Figure 9 A''', C''', D''', Table 2). In contrast, the BMP2 treated organoid had Sox2 positive cells suggesting a cloacal-like tissue, possibly similar to the Cdx2 negative anal canal, or urethra (Figure 9B, B''', Table 2). In summary, BMP2 treated organoids were posteriorized as measured by HoxA13 and HoxD13, had regions of Sox2 expressing cells that were also Pdx1 negative, mixed with Cdx2 expressing cells that were Pdx1 negative. This supports the conclusion that BMP2 treated spheroids are posterior hindgut and can give rise to patterned cloacal tissues.

To investigate if BMP treated organoids have the competency to form more mature cloacal derivatives, we cultured 28d organoids for another 28 days, for a total of 56 days of culture. Maturation of these organoids lead to identification of more mature lineage markers derived from cloaca. At 56 days of age, both BMP4 and BMP2

organoids contain cells that express Uroplakins, Upk1a and Upk2, markers of differentiated urothelial tissue, such as bladder (Figure 10 A, B, I, J, Table 2). BMP7 and EGF treated cultures were unable to produce Upk1a expressing cells, nor induce expression of Upk1a or Upk2 by qPCR (Figure 10 C, D, I, J, Tables 2, 3, 4). As anticipated the more posterior organoids, as identified by HoxA and HoxD13 were still expressing these transcripts at much higher levels than BMP7 and EGF control organoids (Figure 10 E, F). However, only BMP2 treated organoids showed any up-regulation of Sox2 expression, suggesting that BMP2 is more likely to promote a urethral or anal canal fate as compared to the other ligands (Figure 10 G). Other differentiation markers, such as Nkx3.1, a marker of prostate, did not show any significant up-regulation by any of the BMP ligands tested (Figure 10 H). Though at 28 days BMP2 was the only ligand to produce cloaca-like tissue, by 56 days BMP4 treated organoids began expressing some of the more mature cloaca derivatives markers, like Upk1a (Table 2). This suggests that some cloaca progenitors competent to form urothelium were present at 28 days.

As indicated by the large error bars in the qPCR results, all organoids can vary significantly in the epithelial composition, as some organoids treated with BMP2 from this experiment showed an epithelium composed of Pdx1/Cdx2 double positive cells (Supplemental Figure 4). The variability seen in BMP2 organoids is not uncommon, and could be due to a variety of factors. This variation is also apparent at 56 days, where again, many organoids analyzed contained Pdx1/Cdx2 double positive cells in all treatment conditions (Supplemental Figure 5). The variability in organoids could be due to incomplete posteriorization of early stage spheroids. For example, 3 or 4 days in

Chiron/FGF4 might not be sufficient to uniformly posteriorize all the spheroids. For this reason we investigated if increasing the time of exposure to the posteriorizing effects of FGF4 and Chiron might be better for broad and irreversible posteriorization of spheroids. Moreover, we questioned if these spheroids would be more competent to consistently form cloacal organoids.

#### *Temporal effects of Chiron/FGF4 to further posteriorize tissue*

Due to issues with organoid variation we hypothesized that treating our DE with Chiron/FGF4 for a longer period may produce a more homogeneously posterior starting tissue, which would thus be more apt to consistently generate a cloacal tissue. The typical protocol for organoid differentiation calls for collecting spheroids after 3-4 days of Chiron/FGF4 (Summarized in Figure 11A, McCracken 2011). We therefore investigated if longer Chiron/FGF4 would yield more posterior organoids. Starting with a DE monolayer, expressing mostly Sox17/FoxA2 double positive cells we treated with Chiron/FGF4 and collected spheroids from 4-7 days of treatment (Figure 11A,B,D). We confirmed that the cultures were posteriorized by staining the monolayer to verify strong Cdx2 staining in the FoxA2 positive endoderm (Figure 11 C). Spheroids produced from 4-7 days were approximately the same size, though the number of free floating spheroids does decrease with time as monolayers become more three dimensional (Figure 11 D, Supplemental Figure 6). As hypothesized HoxA13 and HoxD13 levels increase considerably with longer exposure to Chiron/FGF4, suggesting that they become more posterior hindgut (Figure 11G, H). This increase is not merely due to aging the spheroids, since 4 day spheroids grown for an additional 2 days in media

lacking Chiron/FGF4 did not show an increase in HoxA13 or HoxD13 (Supplemental Figure 11). Interestingly, Sox2 levels remained similar in day 4, day 5 and day 6 spheroids, but increased at day 7, perhaps suggesting that these more posterior spheroids begin to have early cloacal Sox2 expression (Figure 11F, Figure 1).

*Investigating the synergistic effects of Chiron/FGF4 and both BMP timing and concentration to posteriorize tissue*

Longer exposure to Chiron/FGF4 promotes a more posterior fate. Moreover, adding a treatment with BMP2 also promotes posteriorization. This suggests that FGF, Wnt and BMP have additive effects on posteriorization. Therefore, we then investigated the effects of extending the time of the Chiron/FGF4 and subsequent exposure to BMP2 on patterning the growth of spheroids. Spheroids treated with 5 days of Chiron/FGF4 are called d5, spheroids in 6 days of Chiron/FGF4 are d6, and spheroids treated with 7 days of Chiron/FGF4 are d7. After isolation from the respective days, spheroids were then treated with BMP2 or control/EGF for an additional 5 days and analyzed at 28 days by qPCR looking at the posterior Hox genes. d5 spheroids had far less HoxA13 and HoxD13 expression levels compare to d6 or d7, though d6 appears to have the highest levels (EGF, BMP2 at 100ng/mL) (Figure 12 B). The addition of BMP2 to spheroids had a synergistic effect on posteriorization as indicated by the increase in relative expression levels of HoxA13 and HoxD13 in BMP2 treated organoids compared to EGF controls (Figure 12B bottom row). We also observed a reduction in growth of d7 Chiron/FGF4 organoids, and this is one possible reason for the reduction in posterior factors (Hox13 genes) (Figure 12A). In general, spheroids treated with Chiron/FGF4 for

longer amounts of time (d6 and 7) fail to thrive in culture in contrast to d3-5 generated spheroids (Figure 12A, Supplemental Figure 8A). These data suggest that FGF/Wnt/BMP pathways act to promote a posterior fate, but also have deleterious effects on growth of posterior organoids.

Looking further at the synergistic effects of posteriorizing factors, we hypothesized longer treatment with BMP2 may yield more reproducible cloacal-like tissue as the result of enhanced posteriorization. Therefore, we isolated d4 spheroids (spheroids treated with 4 days of Chiron/FGF4) and treated with seven days of BMP2. We compared these organoids to the d3 spheroids cultured in three days of BMP (discussed in Figures 7-10). These spheroids, d3 and d4, were collected off the same differentiated DE and Chiron/FGF4 treated monolayers so the only variable is days in Chiron/FGF4, and additional BMP treatment. Morphological differences were apparent at both 28 and 56 days in culture in all conditions, including controls, further suggesting there is an intrinsic difference in a d3 and d4 spheroid (Figure 13 A, B). Overall d3 spheroids gave rise to more complex epithelial morphology compared to d4 spheroids, which appeared to contain more mesenchyme (Figure 13 A,B Supplemental Figure 10A,B). In addition to morphological differences, analysis by qPCR confirmed that additional Chiron/FGF4 and BMP treatment synergistically posteriorized the organoids as confirmed by expression levels of HoxD13. Seven day BMP2 treated d4 spheroids have much higher levels of HoxD13 than the d3 spheroids treated with three days of BMP2 (Figure 13C). Also, more mature markers, like Upk1a are also more pronounced in the seven day BMP2 d4 spheroid treated cultures (Figure 13D, supplemental figure 7). Upk1a can be detected by immunostaining in the 7 day BMP2 d4 organoids at 56

days confirming the qPCR expression data and presence of mature urothelial cells (Figure 14).

We hypothesized another way to reproducibly generate posterior tissue capable of becoming cloaca could be to treat spheroids with higher concentrations of BMP ligand. Therefore we tested if higher concentrations of BMP2 increased levels of posterior Hox genes and cloaca markers. We took d5 spheroids (from 5 days of Chiron/FGF4) and split them into three groups, controls treated with EGF, BMP2 at 100ng/mL, and BMP2 at 500ng/mL. We analyzed three organoids per condition at 28 days by qPCR. Interestingly, Cdx2 expression went down in a stepwise fashion with EGF/control organoids expressing the highest levels and BMP2 at 500ng/mL expressing the lowest levels of Cdx2 (Figure 15 A). HoxA13 and HoxD13 both showed increases in BMP2 treated organoids at both concentrations compared to control, though only HoxA13 showed a significant increase in expression from low BMP2 (100ng/mL) to high BMP2 (500ng/mL) (Figure 15 C,D, Tables 3 & 4). This suggests that the higher concentration of BMP2 results in a higher degree of posteriorization, and the decrease of Cdx2 expression is likely the result of differentiation. This differentiation is indicated by the up-regulation of Sox2 observed in the high BMP2 (500ng/mL) treated organoids, suggesting that the higher dose of BMP2 may be promoting a urethral or anal canal fate (Figure 15B, Table 3). Another potential marker of differentiated urothelial tissue is Gata3, which has known involvement the proper connecting of the nephric ducts to the urogenital sinus (Chia 2011). Looking at Gata3 by qPCR in these 28 day organoids suggests that in almost a stepwise fashion BMP2 at 100ng/mL induces expression of Gata3 over EGF controls, but this is increased further in

500ng/mL BMP2 organoids, suggesting that higher concentrations of BMP2 may be leading to urothelial tissue differentiation, which is also supported by the increase in Upk1a (Figure 15 E, F, Tables 3 & 4). All in all, the data suggests that both additional time in Chiron/FGF4 and extended time in BMP, or increased BMP concentration have synergistic posteriorizing effects (Supplemental Figure 9).

## **Discussion**

### *Studying cloaca using an in vitro human modeling system*

The urogenital and anorectal systems arise from a complex developmental process, that when altered leads to clinically significant malformations. Though studies have shown that pathways such as FGF, WNT, and BMP play roles in formation of posterior tissue, a thorough understanding of the development of cloaca, from the specification of progenitor cells through differentiation of mature lineages does not exist (Zorn & Wells 2009). Studies of human cloacal development are impossible because it is not currently feasible to prospectively identify fetuses with early cloacal malformations. Thus we felt that it was important to generate an experimental system from which cloacal-like tissues could be generated from hESCs. Such a system would allow for unprecedented studies of cloaca development and identification of molecular pathways that are affected in patients with anorectal and urogenital malformations. Although our success in reproducibly generating a cloacal tissue in culture was variable, we have been able to show that under the right conditions generation of cloacal-like tissue is possible. In addition our identification and use of new molecular markers of the developing cloaca has made it possible to study early patterning and cloacal organ

development in mouse. In particular, these markers for cloaca and its derivatives have allowed us to identify developing cloacal cell populations in human PSC-derived cloacal organoid cultures.

Our analysis of mouse embryos has shown that K8, Sox2, and FoxA2 can be used together to successfully mark certain populations of cloaca and its early derivatives. We propose that early Sox2+/FoxA2+ cells mark a dorsal cloacal progenitor located in the distal hindgut and with K8 can be used to temporally and spatially look at cloaca development progression. Once the cloaca cavity has been established at e10.5 in the mouse embryo a gradient of K8 is observed. It appears that highly expressing K8 cells on the anterior and ventral side of the cloacal cavity will go on to become the UGS, which stays K8 positive. Whereas the cells at the dorsal posterior end of the cavity that are K8 weak and strongly expressing Sox2, go on to expand ventrally, and then once septation has occurred these strongly positive Sox2 cells become urethra, or anal canal. Having established this pattern of expression we now can analyze organoids for cloacal like tissue prior to expression of more mature markers like uroplakins, Nkx3.1, and androgen receptor (AR). This will be extremely valuable in all studies of cloacal malformation and development.

#### *Variability of human organoid cultures*

We have observed significant variability in patterning of PSC-derived organoids, both between organoids from the same experiment, and from experiment to experiment. There could be a number of factors causing variability, such as variability of growth factor activity, lack of a required factor, or variability of starting spheroid tissue. Our data

suggests that inconsistency in the early spheroids can have an impact on the patterning of organoids. We believe that as hundreds of spheroids bud off the monolayer it is possible that they are at slightly different levels of posteriorization. For example, one spheroid may be highly expressing Cdx2, and another may have only just begun up regulation of that transcription factor. This difference at the earliest step in organoid generation could explain the variation we see at both 28 and 56 days. The slightest variation could result in spheroids that react differently to BMP treatments simply due to different transcription factors being expressed when we attempt to pattern them. The variation we observe is also evident when we look at all BMP treated organoids compared to EGF controls as a group, in tables 2, 3, and 4. Here it is apparent that the increases we see in BMP2 and BMP4 treated organoids are trends (Table 3), yet only a portion of these experiments are statistically significant as a result of variation (Table 4). Therefore, we believe further investigation into exposing spheroids to longer Chiron/FGF4 treatment could be one solution. Our data suggests that longer treatment increases posteriorization of spheroids. Increasing the posteriorization of spheroids through longer treatments could result in transcription factor expression profiles that are more uniform and reproducible. Ideally, if we could produce spheroids that are synchronized from the beginning they should react in the same manner to BMP treatments, and likely yield more consistent results. Therefore, further study into synchronizing the hindgut spheroids is a priority.

In addition to variation we believe is the result of inconsistencies in early patterning, we also observed variation in the effects of different BMP ligands. As described above and summarized in Tables 2, 3, and 4 we see markers of cloacal-like

tissue in some BMP2 and BMP4 treated organoids and trends of increased posteriorization as measure by hox genes, whereas BMP7 treated organoids showed little increases in posteriorization but no expression of other markers. These differences could be due to dissimilarities in ligand activity, ligand/receptor affinity or specificity. For instance, the ED<sub>50</sub> (effective dose) of each BMP ligand is different (R&D Systems). Therefore, though we used the same concentration of BMP2, 4, and 7 in each experiment the effective dosage varies significantly and could result in the observed differences. In addition it is known that BMP ligands 2 and 4 belong to the same subgroup, but BMP7 belongs to a subgroup known as the growth and differentiation group (Ramel 2012). Not only do these ligands belong to different subgroups within the family, they also can signal through different BMP receptors. Although BMP2, BMP4 and BMP7 signal through most of the same type I and type II receptors, these receptors are capable of forming various receptor combinations. These BMP ligand-receptor complexes can induce different signaling cascades due to small differences in orientation of the type I receptor (Mueller 2012). It is known that BMP ligands have different activities not only due to dosage, but differences in activation of signaling cascades as a result of the many ligand-receptor complex combinations. These differences in activity and or signaling are areas that need further investigation.

### *Signaling pathways to investigate further*

One powerful use of an *in vitro* organoid system for studying cloaca is to systematically test signaling pathways, such as Shh and BMP, for their involvement in cloacal development. For instance, based on several studies showing BMP7 is

important for septation to occur properly we proposed BMP7 treated spheroids may produce cloacal-like tissue better than BMP2, which was not what our initial data supported (Wu 2009, Xu 2012). In fact based on our preliminary work it appears that BMP7 does not posteriorize endoderm to promote cloacal-like tissue, rather based on morphology it appears to promote mesenchymal growth over the growth of the epithelial components of the organoid. Interestingly, due to the known role of BMP7 to promote apical basal polarity of division in the mesenchyme around the endoderm lined cloacal cavity (Xu 2012), it seems consistent that BMP7 may have promoted mesenchyme expansion in our early treated cultures. One might suspect that if spheroids were initially treated with BMP2 to posteriorize that BMP7 added to cultures after generation of a cloacal tissue could promote differentiation processes that occur during septation.

TGF $\beta$  may also play a role in differentiation of cloacal derivatives into mature organs. From studies in mice, it appears that Smad2 and Smad3 may be critical during bladder formation, specifically in mediating smooth muscle differentiation (Islam 2013). Interestingly we did not see much smooth muscle differentiation in our cultures (data not shown), and this could potentially be from lack of proper growth signals, such as TGF $\beta$ . The cloacal organoid system could be used to test this hypothesis through manipulation of TGF $\beta$  signaling factors at later stages of organoid development in attempts to increase in urothelial differentiation.

Other known vital signaling pathways could be carefully investigated using the organoid culturing system, such as Shh. The *in vitro* system allows for manipulation of Shh signaling at various stages of development through the addition of Shh protein or by blocking Shh with cyclopamine. The addition or removal of Shh signaling in the

culture system at precise times could be a key factor in our ability to produce specific lineages derived from cloaca. Though Shh is known to play vital roles in genital tubercle outgrowth and septation, it may play unknown roles at other stages of cloacal development such as early cloacal patterning, lineage fate decisions, or during maturation, which could be tested in the *in vitro* culturing system (Seifert 2009, Seifert 2010). For example, we recently identified an early cloacal patterning defect in Shh knockout mice (Runck submitted), and hypothesize that hedgehog plays a similar role in patterning the human cloaca. For example, Shh's role in regulating transcription factors such as Sox2 in cloacal development could be carefully investigated.

Anophthalmia-esophageal-genital (AEG) syndrome is a disease where patients present with either small eyes (microphthalmia) or lack of an eye (anophthalmia), oesophageal atresia with or without tracheo-oesophageal fistula, and urogenital malformations (Shah 1997). Not surprisingly this syndrome is associated with mutations in Sox2, as Sox2 is known to be important in eye development, is vital to the foregut, and is expressed in cloacal endoderm (Williamson 2006). Fistulas between the esophagus and trachea often form when there is a lack of Shh signaling, which also often leads to cloacal abnormalities. Interestingly, Sox2 expression is maintained in the foregut of Shh<sup>-/-</sup> embryos yet in the cloaca of Shh knockouts Sox2 expression is lost (Williamson 2006, Runck Submitted, and Figure 4). This discrepancy could be due to differences in regulation of Sox2 in foregut versus hindgut, but suggests that the regulation may be lineage dependent. Manipulation of Shh signaling in the human organoid modeling culture would allow investigation of Sox2/Shh interactions at a molecular level.

Lastly, studies in mice suggest that FGF signaling plays a vital role in cloacal development. This could be investigated using the human *in vitro* culturing system. Loss of FGF10 in mice does not really impede septation, however, the animals actually lose rectal epithelial tissues (Fairbanks 2004). Thus, addition of FGF10 to the organoid culturing system may enrich for anal canal or rectal tissue.

Overall, there are multiple signaling pathways that are important for proper cloacal development, septation, and maturation of cloacal derivatives. The organoid culturing system would allow each of these pathways to be carefully manipulated to determine requirements for generation of certain cloacal lineages. It is likely that each cloacal derivative requires different amounts of active signaling from various pathways described for proper development and maturation. Using this system to carefully dissect out the requirements of FGF, Shh, BMP, and Wnt signaling for proper development of cloaca and its mature derivatives will not only be valuable, but will overall give better understanding to congenital defects of the urogenital and anorectal systems.

#### *iPSCs to study human cloacal malformations*

Quite possibly the most powerful aspect of this research is the ability to use this culturing system to study human cloacal disease *in vitro*. With recent advances in generating induced pluripotent stem cells (iPSCs) from patient samples, one could study defects in patients with anorectal or urogenital malformations in a dish. Studying patient cells for cellular dysfunction, improper signaling, and ability to generate mature tissues are all possible with the *in vitro* modeling system. iPSCs generated from patients with cloaca malformation, for example, could be used to identify signaling components

missing that lead to the malformation, and then adding those factors into the culture in attempts to “force” septation. Having a more comprehensive understanding of these malformations will hopefully lead to better treatment options in the future.

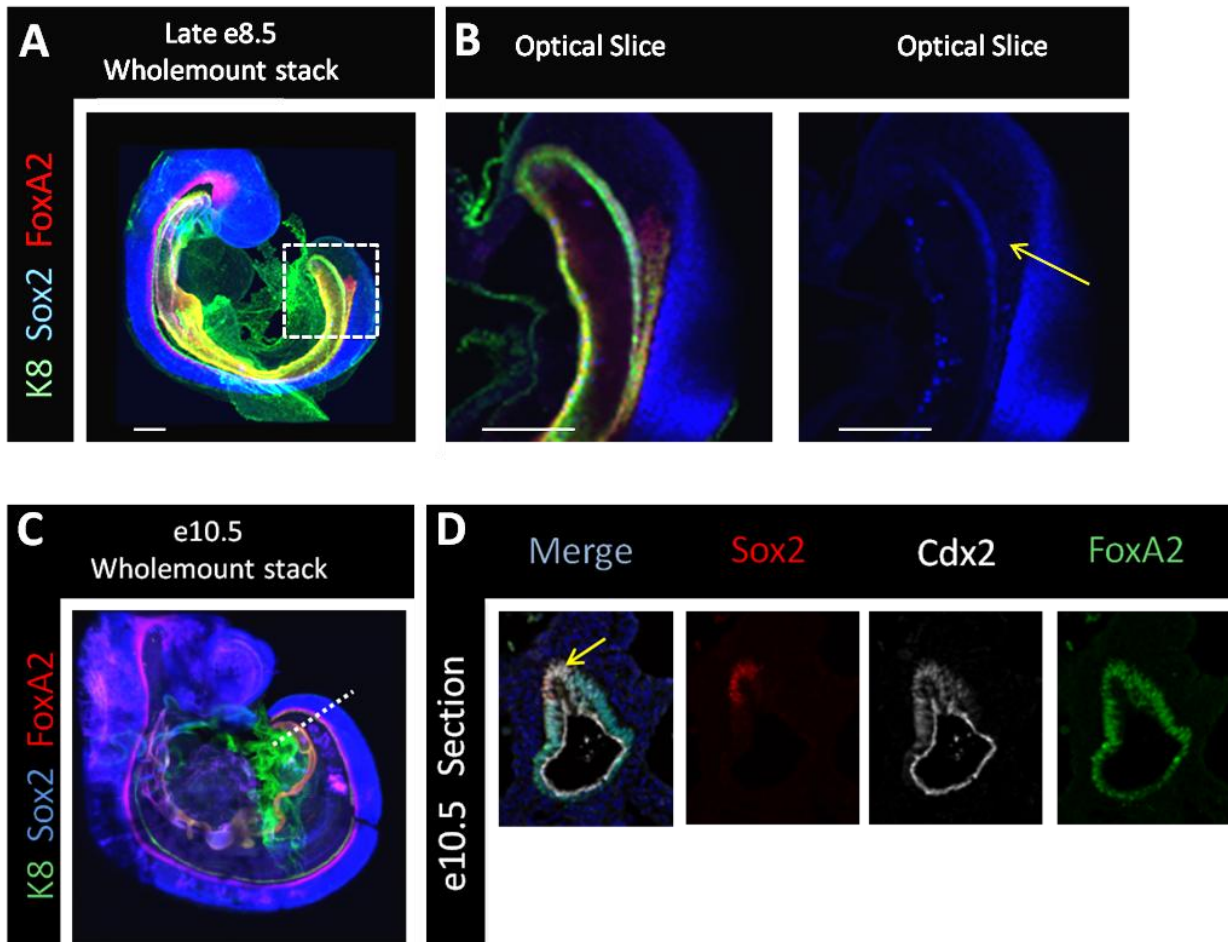


**Figure 1. Novel Sox2 expression in distal gut at e8.5 and Sox2/Cdx2 co-expressing cells at e10.5**

(A) Whole mount staining (n=3) on late e8.5 mouse embryo shows Sox2 (blue) expression in the hindgut endoderm, magnification (B). Cells are also FoxA2 positive and show expression of K8. (C) whole mount staining on e10.5 embryo (n=3), paraffin section through posterior hindgut (approximately hind limb level). (D) Highlights co-expression of Sox2 (red) and Cdx2 (white) within FoxA2 (green) endoderm lining the gut tube.

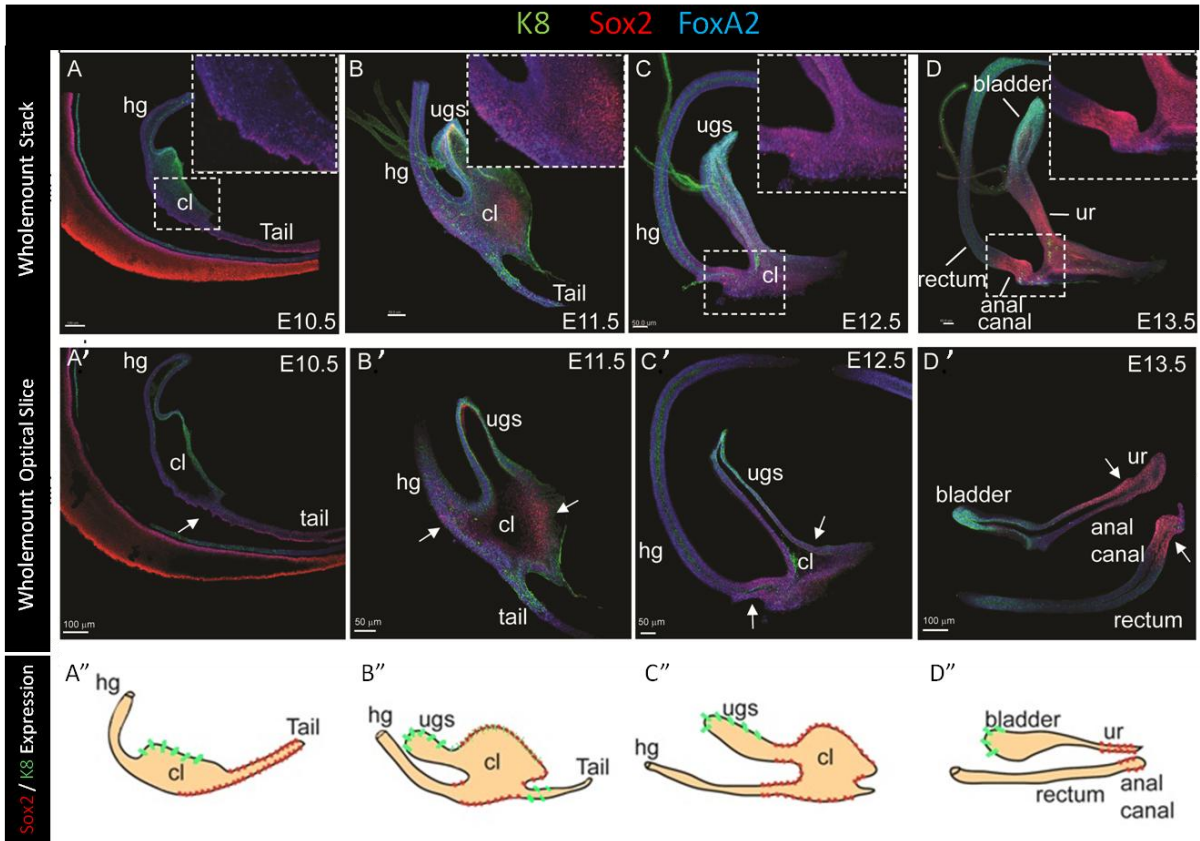


**Figure 2. Expression pattern of cloacal markers K8, Sox2, and FoxA2 in wild-type mouse embryos**

(A-D) Whole mount immunohistochemistry of K8 (green), Sox2 (red) and FoxA2 (blue) in embryos e10.5-e13.5. (A'-D') optical slices from whole mount. (A''-D'') Diagram of K8 and Sox2 expression in cloaca. (A,A', A'') Expression pattern of K8 and Sox2 is spatially defined at e10.5 with K8 in the anterior ventral cloaca and Sox2 lines the dorsal posterior cloaca and tail gut. (B,B',B'') K8 intensity increases at e11.5 and also highlights the ureters, Sox2 expression expands ventrally to line most of the cloacal cavity. (C,C',C'') K8 expression intensifies in the urogenital sinus at e12.5, as does Sox2 expression in the anal canal and the developing urethra. (D,D',D'') By e13.5 septation has completed and the K8 expression is restricted to the developing bladder, and Sox2 lines the now separated urethra and anal canal. N=3 for each embryonic stage. (Amended From: Runck et al. Submitted)

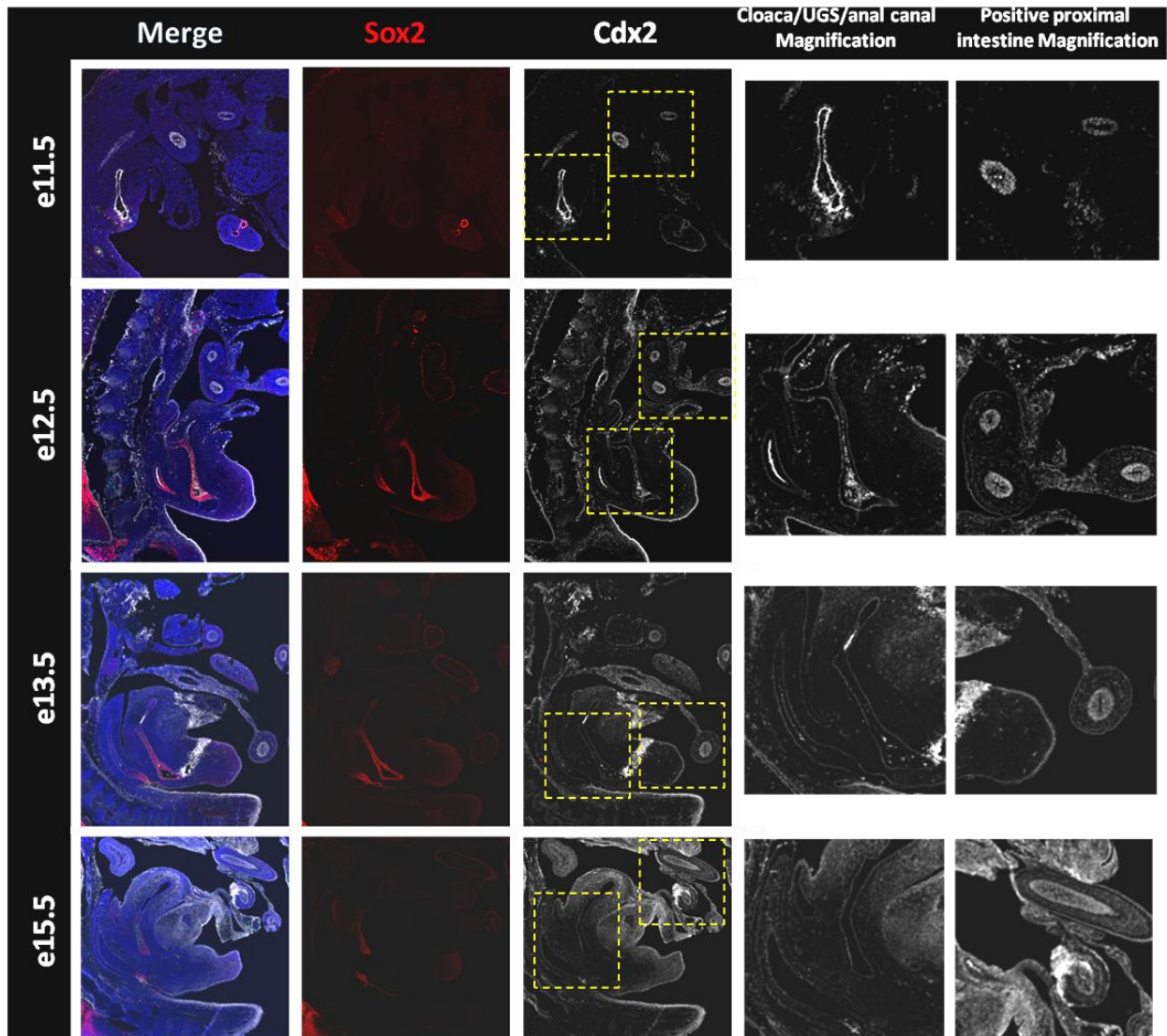


**Figure 3. Cdx2 is not observed in the cloaca from e11.5-e15.5**

Series of paraffin sections of mouse embryos at e11.5, e12.5, e13.5 and e15.5 with immunofluorescent analysis of Sox2 (red), Cdx2 (white) and nuclear stain dapi (blue). Sox2 is not co-expressed with nuclear Cdx2 at any stage analyzed. Magnifications (far right) highlight lack of specific Cdx2 staining in cloaca (e11.5-e12.5) and rectum (e13.5, e15.5) but positive nuclear Cdx2 is observed in more proximal intestinal rings at all stages. n=3 per embryonic stage.

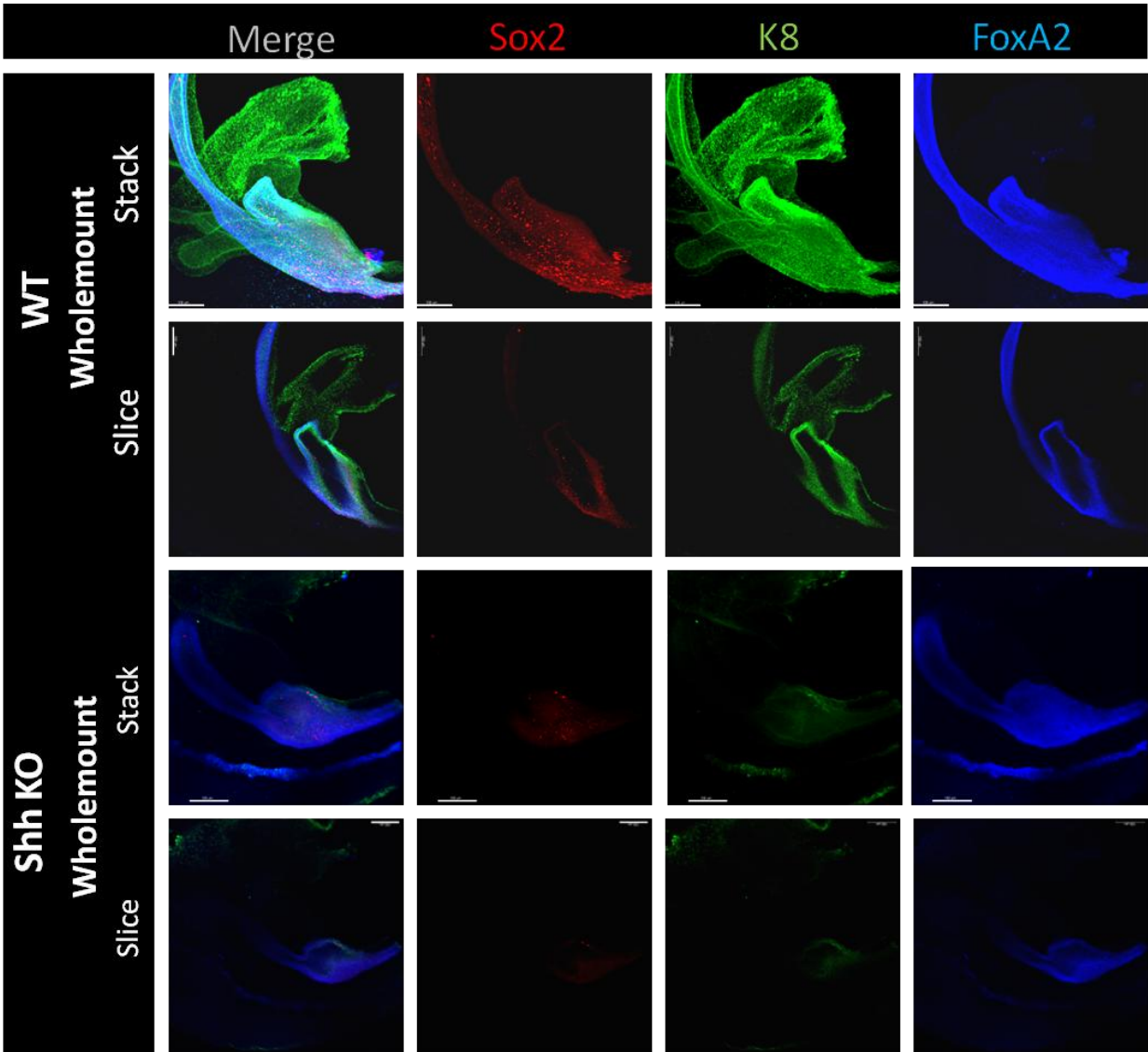


**Figure 4. Shh KO embryos have loss of Sox2 and K8 in the cloaca**

Analysis of mouse embryos at e11.5. Top two rows show wild-type (WT) embryos n=3 (top whole mount stack, bottom optical slice), bottom two rows are Shh KO embryos n=3 (top whole mount stack, bottom optical slice). WT embryos show strong staining of Sox2 (red), K8 (green), and FoxA2 (blue) throughout the cloacal cavity as expected. Shh KO mouse embryos show loss of Sox2 and severe reduction/loss of K8 in the cloacal cavity. (Runck et al. Submitted)

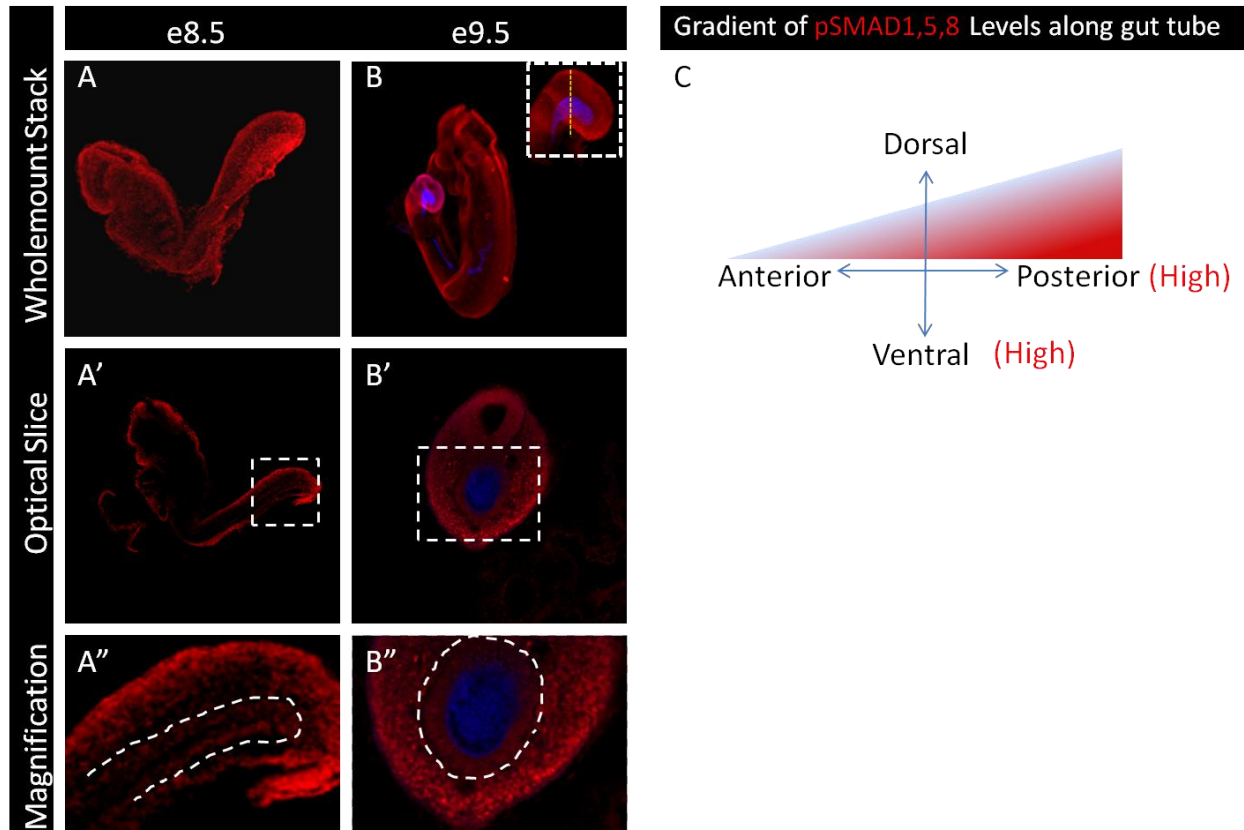


**Figure 5. Active BMP signaling is observed in a gradient along the A-P and D-V Axes**

(A) Whole mount pSMAD1,5,8 staining (red) on e8.5 embryo (n=2) shows strong staining along the neural tube as well as in the posterior hindgut. (A') Optical slice through e8.5 highlights intense posterior staining in mesenchyme and in endoderm of hindgut. (A'') magnification of e8.5 hindgut. (B) Whole mount immunostaining of e9.5 embryo (n=1) showing strong nuclear pSMAD1,5,8 (red) staining in tail (blue is non-specific Cdx2). (B') Optical slice shows gradient of intense nuclear staining in dorsal neural tube, in addition to strong nuclear staining in a graded fashion with most intense staining in ventral mesenchyme. (B'') magnification of endoderm shows weak nuclear staining. (C) Diagram of observed gradient of active BMP signaling, measured by pSMAD1,5,8, with highest expression in the hindgut in the posterior ventral domain.

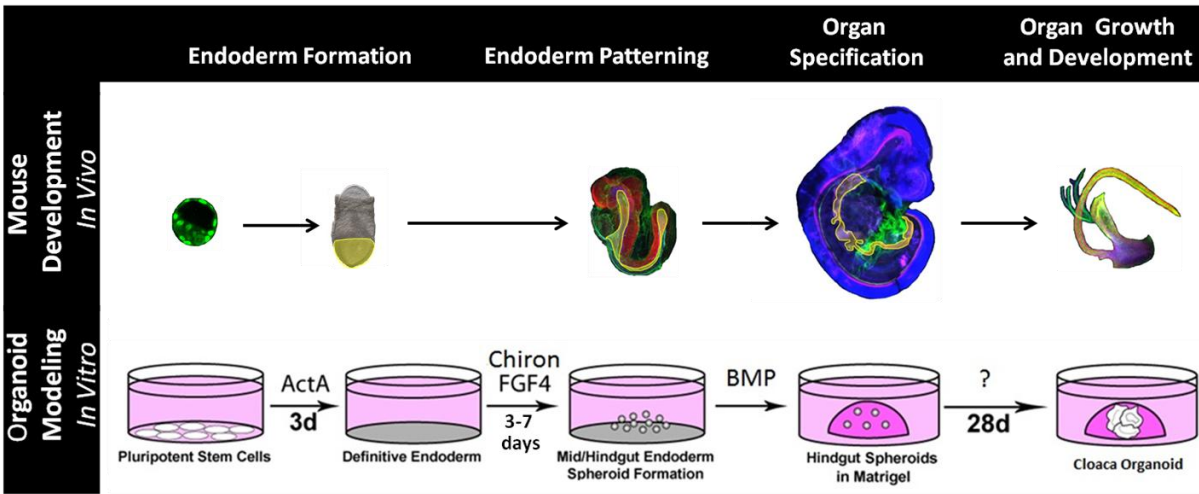


**Figure 6. Using hESC Organoids to model development of the cloaca**

Compares mouse *in vivo* development (top row) to *in vitro* organoid modeling system (bottom row) from endoderm formation (left) through organ specification and development (right). Blastula stage embryo transition to gastrula stage is similar to conversion of human pluripotent stem cells (hPSC) into definitive endoderm (DE) by 3 days of Activin A treatment. Endoderm patterning occurs from DE formation in a gastrula stage embryo to e8.5 mouse embryo, which is similar to Chiron/FGF4 patterning in culture to produce spheroids. Additional treatment with growth factors like BMP promotes organ specification, similar to specification occurring in e10.5 mouse embryos. Further culturing of organoids allows for maturation and development of tissues which are reminiscent of late stage mouse embryos or postnatal tissues.

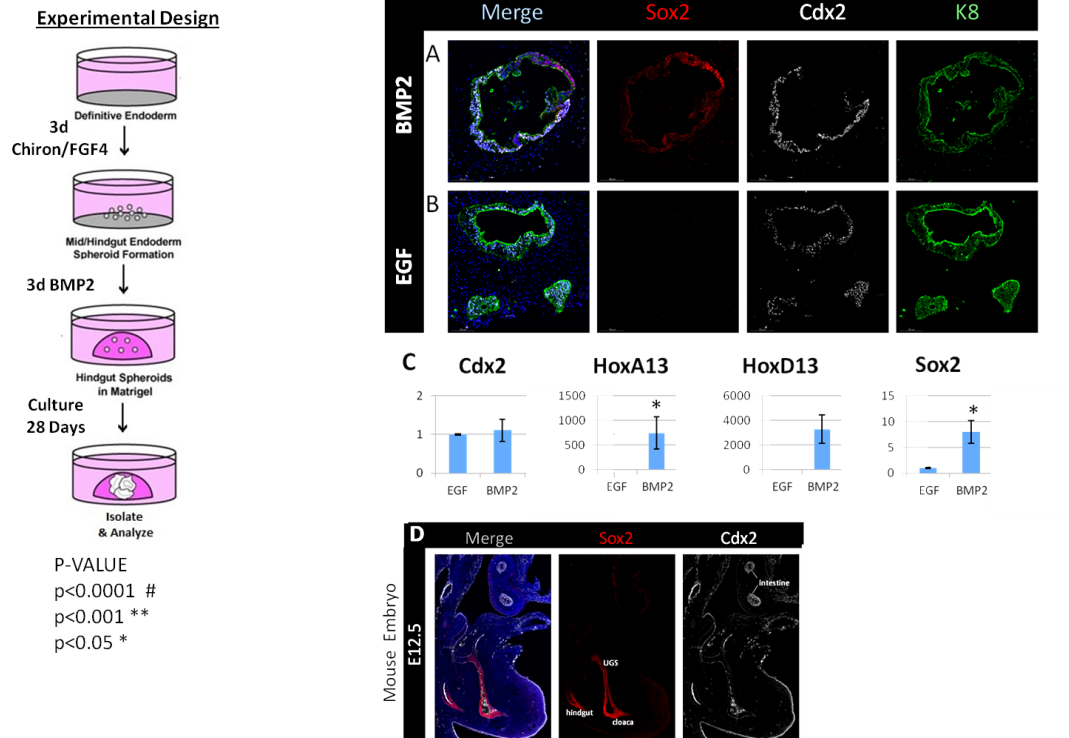


**Figure 7. Generation of cloacal tissue with BMP2**

Spheroids were taken after 3 days of Chiron/FGF4 treatment, embedded in matrigel, treated with EGF or BMP2 (100ng/mL) for 3 days and cultured for a total of 28 days. Analysis of organoids by immunohistochemistry shows that (A) BMP2 treated organoids express Sox2 (red), which is separate from Cdx2 (white), and all epithelial rings express K8. Whereas, (B) control treated EGF organoids do not express Sox2, showing only Cdx2 and K8 positive epithelium. (C) Analysis by qPCR at 28 days shows expression of Cdx2 is similar, however increases in expression were observed in BMP2 treated organoids over controls for HoxD13, and statistically significant increases over controls for HoxA13 and Sox2. (D) Staining expression of BMP2 organoids (A) is reminiscent of e12.5 mouse embryos, which show Sox2 expression in the cloaca and anal canal are completely separate from Cdx2 expression observed in more proximal regions of the intestine. Student t-test analysis was used to determine statistical significance,  $p < 0.05$  \*, compared to EGF controls.

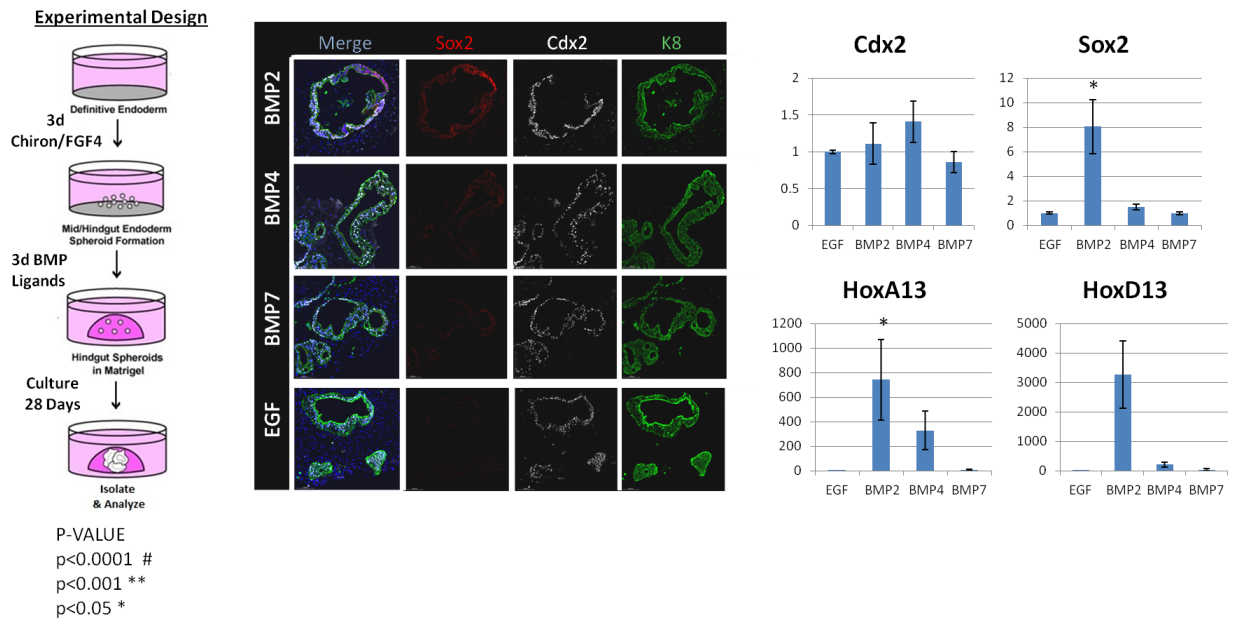


**Figure 8. Comparison of BMP ligands in generating cloacal tissue**

Analysis of BMP ligands on spheroids generated from 3 days of Chiron/FGF4, 3 days of BMP ligand, and cultured for a total of 28 days. BMP2 ligand data and control is the same data from Figure 7. Immunofluorescent staining of Sox2 (red), Cdx2 (white) and K8 (green) compares BMP2, BMP4, BMP7 ligands to control EGF treated organoids. BMP2 treated organoids (top) show some expression of Sox2 within the epithelium. BMP4, BMP7, and EGF organoids show no expression of Sox2. All epithelial tissue is Cdx2/K8 double positive. Analysis by qPCR (right) shows similar levels of Cdx2 expression are achieved by all treatments, however only BMP2 organoids showed up-regulation of HoxD13, and statistically significant increases for Sox2 and HoxA13. BMP4 organoids did show small increases in HoxA13 compared to controls, which was not statistically significant. Statistical significance was determined using student t-test, where BMP treated organoids were compared to EGF controls,  $p < 0.05$  \*.

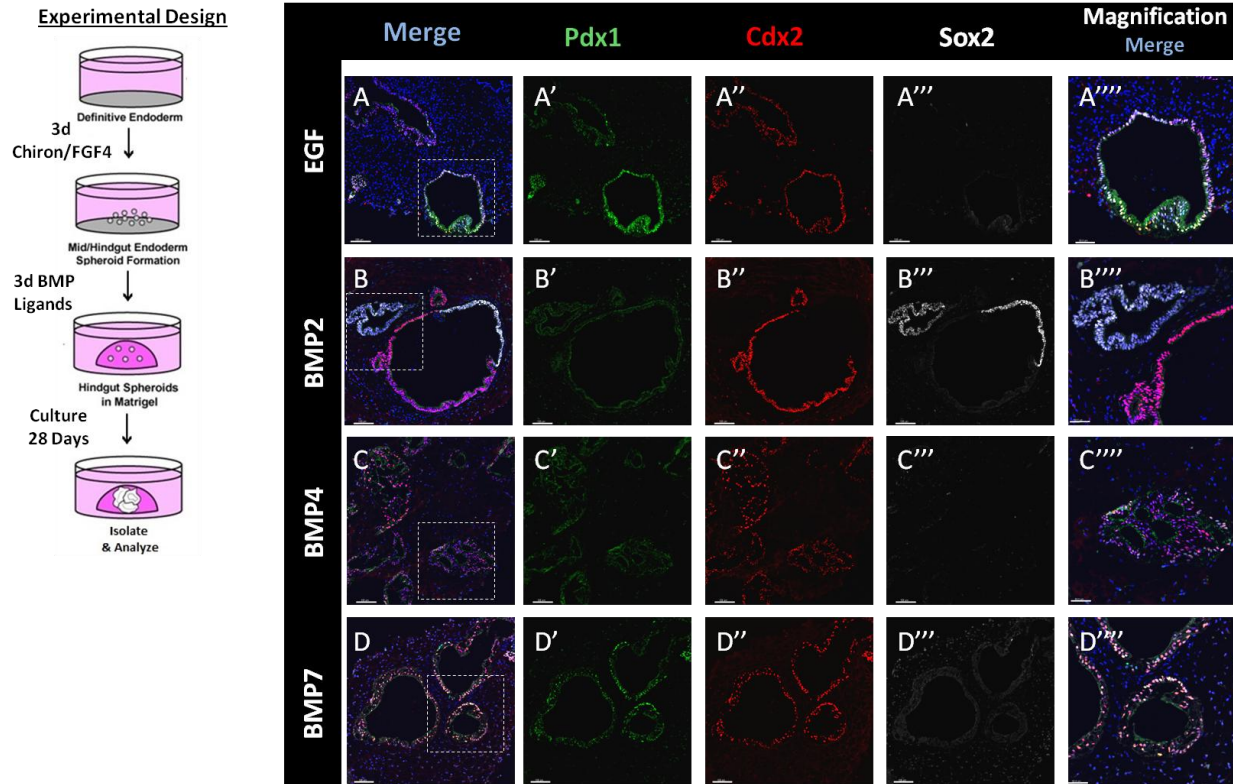


**Figure 9. BMP2 treatment yields distal cloacal-like epithelium**

Further immunofluorescent analysis of organoids from Figure 8. (A-A''') EGF control organoids express epithelium that is Pdx1 (green), Cdx2 (red) double positive suggesting duodenal fate, which is Sox2 (white) negative. (B-B''') BMP2 treated organoids do not express Pdx1 (B'), but show regions of Cdx2 (B'') staining that is separate from Sox2 (B''') expression. (C-C''') BMP4 treated organoids have regions of Pdx1/Cdx2 double positive epithelium and lack Sox2. (D-D''') BMP7 organoids show almost entirely Pdx1/Cdx2 double positive epithelium.

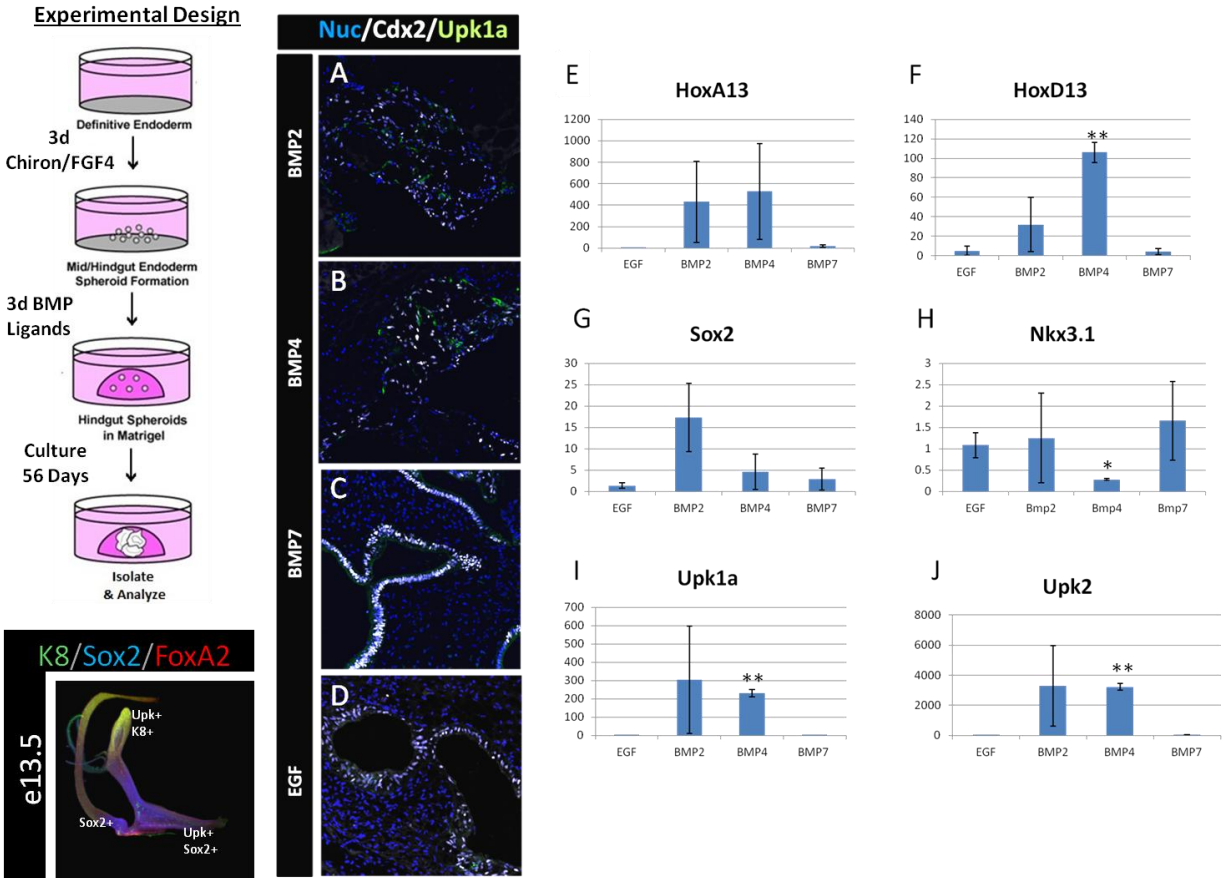


**Figure 10. Induction of mature cloacal markers in response to BMP2 & BMP4, but not BMP7**

Analysis of organoids from Figures 8 and 9 at 56 days after culture. (A-D) Expression of Upk1a (green) and Cdx2 (white) shows Upk1a positive cells are present in both BMP2 and BMP4 treated cultures, but not in BMP7 or EGF controls. (E-J) qPCR analysis of 3 organoids per condition shows increases in HoxA13 (E), HoxD13 (F), Sox2 (G), Upk1a (I) and Upk2 (J) in BMP2 organoids over EGF controls. BMP4 treated organoids showed relative increase in expression of HoxA13 (E), however statistically significant increases in HoxD13 (F), Upk1a (I), and Upk2 (J) were observed. Expression levels of Nkx3.1 were not increased compared to controls (H). Bottom left panel of e13.5 mouse embryo shows septated cloaca has expression of Sox2 that is restricted to urethra and anal canal, Uroplakins are restricted to the urethra and developing bladder, suggesting qPCR data of high Sox2/Uroplakins in BMP2 treated organoids could be due to differentiation towards urethral fate or a mix of urethra, bladder, and anal canal. Student t-test analysis was used to determine statistical significance ( $p < 0.05$  \*,  $p < 0.001$  \*\*) over EGF controls.

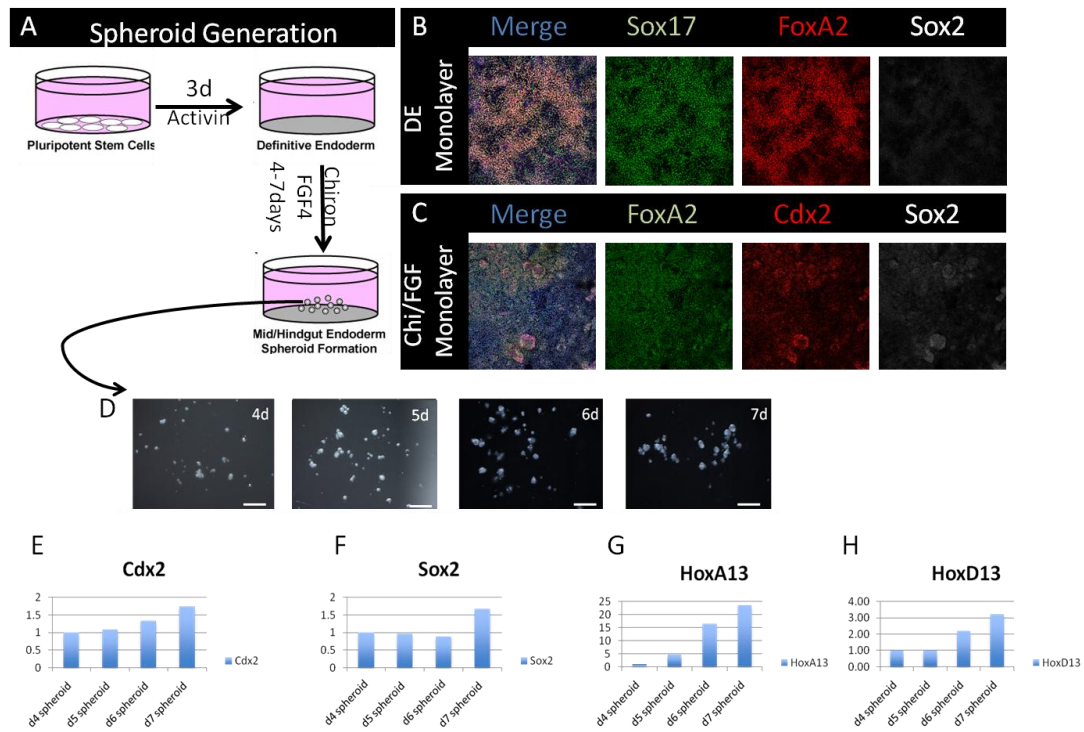


**Figure 11. Temporal role for Chiron/FGF4 in posteriorization of spheroids**

(A) Schematic of spheroid generation to test posteriorizing effects of Chiron/FGF4. hPSCs are treated with Activin A for 3 days to form DE, DE is then treated with 4-7 days in Chiron/FGF4 before collecting and plating spheroids. B) DE monolayer is strongly Sox17 (green)/ FoxA2 (red) double positive. C) Chiron/FGF4 monolayer after 4 days of treatment shows FoxA2 (green) positive endoderm, with strong Cdx2 (red) expression and no Sox2 (white) expression. D) Spheroids isolated from 4-7 days of Chiron/FGF4 treatment are similar in size and morphology. E-H) qPCR analysis of spheroids (pooled 75-100 spheroids per condition) isolated after 4-7 days of Chiron/FGF4 at day 0 (not cultured after harvesting). Relative expression levels of Cdx2 (E), HoxA13 (G) and HoxD13 (H) increase in stepwise fashion as length of Chiron/FGF4 exposure increases. Sox2 (F) exposure stays steady until it slightly increases after 7 days of exposure to Chiron/FGF4.

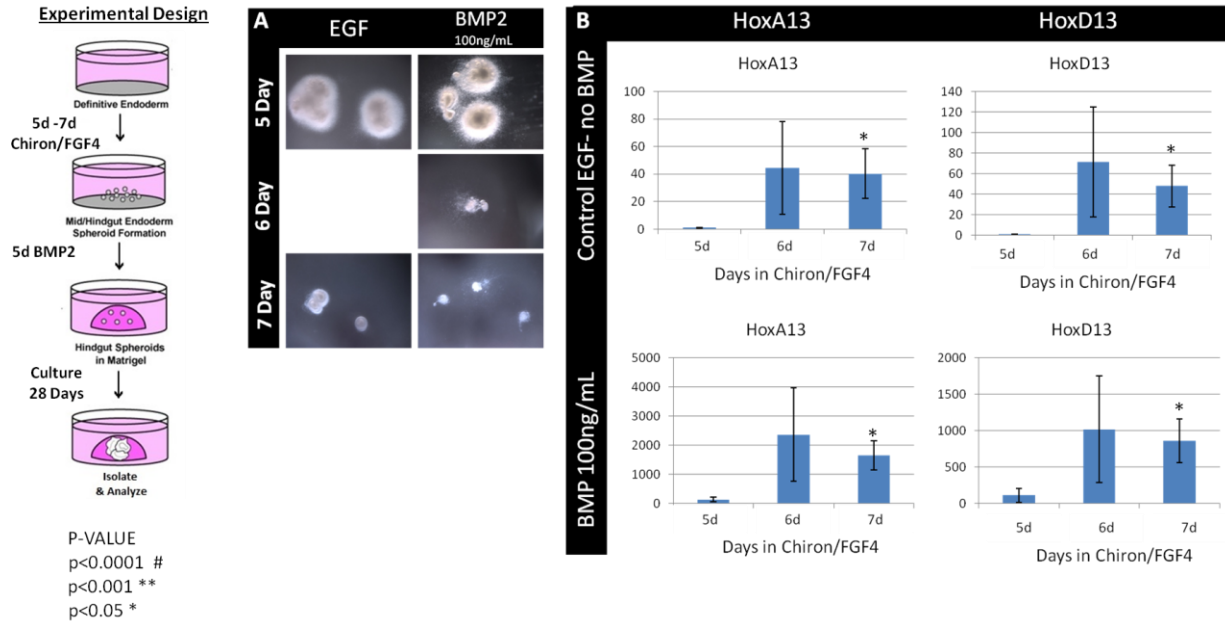


**Figure 12. Longer Chiron/FGF4 treated spheroids are more posterior at 28 days**

Analysis of spheroids after 5-7 days of Chiron/FGF4 treatment, followed by BMP2 or EGF for 5 days and cultured out a total of 28 days. A) Noteworthy differences in size are observed between 5 day spheroids compared to 6 and 7 day. More time in Chiron/FGF4 yields smaller organoids at 28 days. BMP2 treated organoids are smaller than EGF organoids at 28 days. B) qPCR analysis of HoxA13 and HoxD13 in control organoids (top row) and BMP2 treated (bottom row) comparing days in Chiron/FGF4 . Increases in HoxA and HoxD13 are observed in EGF controls in 6d organoids over 5d controls. This increase is statistically significant in 7d Chiron/FGF4 spheroids. Similar effects are observed in BMP2 treated organoids (bottom), with relative expression levels of Hox genes increasing in 6 day Chiron/FGF4 spheroids and sustained, and statistically significant in 7 days. In addition relative levels of gene expression in BMP2 treated spheroids are increased over EGF controls in 5 day, 6 day and 7 day Chiron/FGF4 organoids, though only 7 day Chiron/FGF4 organoids shows statistically significant increases in relative expression with the addition of BMP2. Statistical significance was determined using 5d Chiron/FGF4 EGF organoids as “controls” by unpaired, 1 tailed, student t-tests, where  $p < 0.05$  \*.

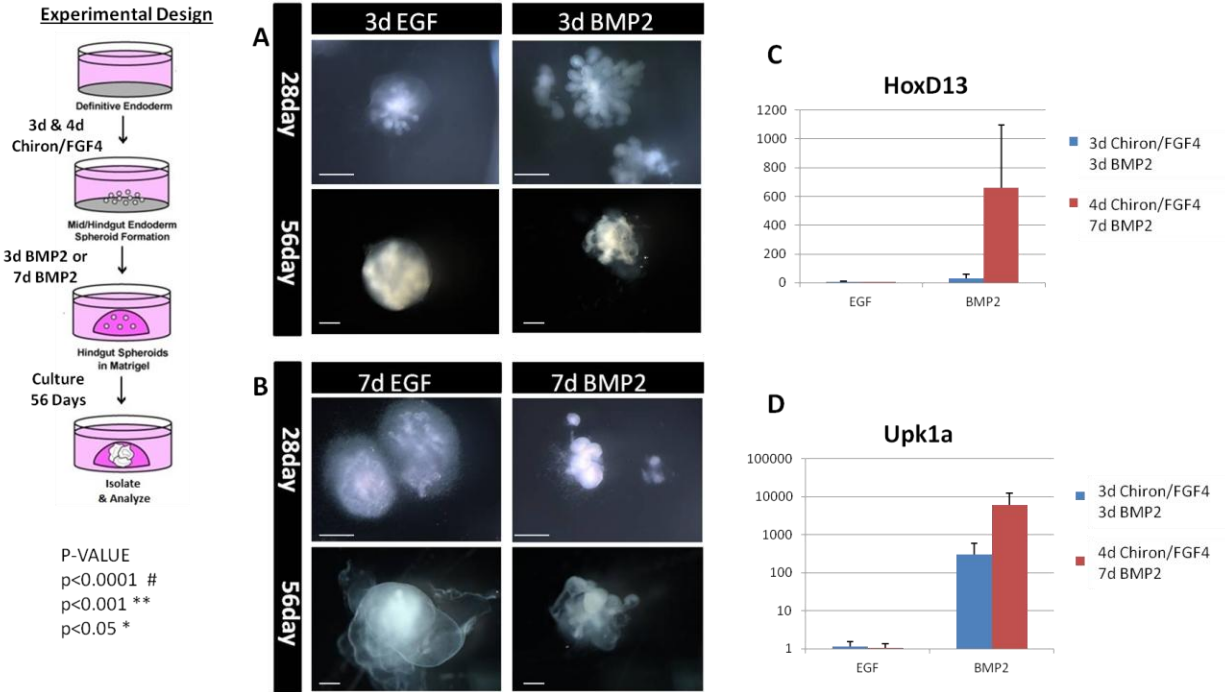


**Figure 13. More Chiron/FGF4 and Longer BMP2 yields more posterior tissue with higher Upk1a expression**

Analysis of organoids from 3 day Chiron/FGF4 with 3 day BMP treatment (data from figures 7-10) compared to organoids generated from 4 day Chiron/FGF4 with 7 days BMP2. A) Morphology of 3 day spheroids treated with 3 days EGF or BMP2 at 28 and 56 days. EGF organoids (left) contain complex epithelial component with a surrounding layer of mesenchyme. BMP2 organoids (right) show complex budding structure with little mesenchyme at 28 days that is somewhat reduced in complexity by 56 days. B) Morphology of 4 day spheroids treated with 7 days of BMP2 at 28 and 56 days. EGF organoids (left) have large amounts of mesenchyme around a simple epithelium. BMP2 organoids (right) are small simple structures with little mesenchyme. C-D) qPCR analysis of organoids at 28 days. C) HoxD13 levels are increased in BMP2 treated organoids over EGF controls. BMP2 organoids generated from 4 day Chiron/FGF4 show much higher levels of expression (red bars). D) Both sets of BMP2 treated organoids have higher expression of Upk1a compared to EGF controls. 4 day Chiron/FGF4 BMP2 organoids (red bars) have higher Upk1a expression than 3 day Chiron/FGF4 BMP2 organoids (blue bars). Increases in relative expression are not statistically significant as determined by unpaired, 1 tail, student t-tests.

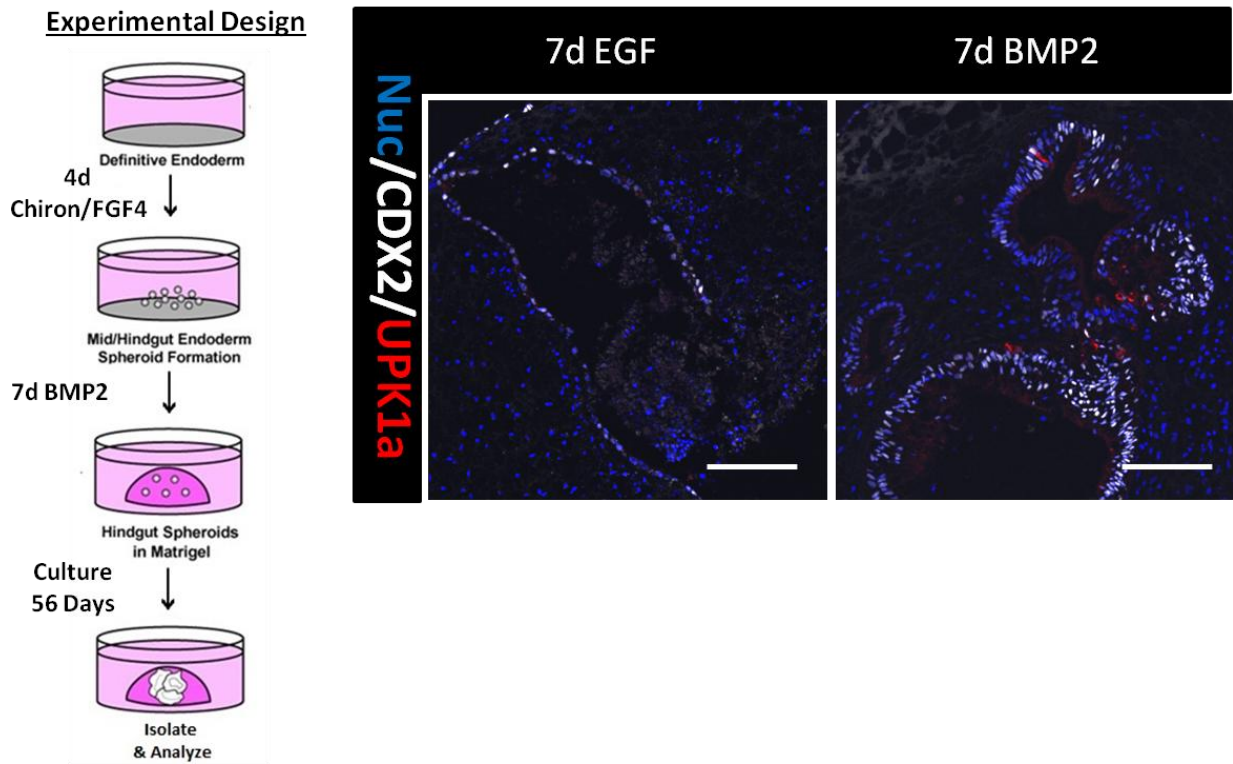


**Figure 14. Maturation and expression of urothelial marker Upk1a**

Immunofluorescent analysis of 56 day organoids generated from 4 day Chiron/FGF4 spheroids and treated with 7 days of BMP2 or EGF (56 day analysis of organoids from Figure 13). Staining of organoids for Cdx2 (white) and Upk1a (red) shows that EGF control organoids (left) do not express Upk1a within the Cdx2 positive epithelium. BMP2 treated organoids (right) express Upk1a within some of the epithelial cells.

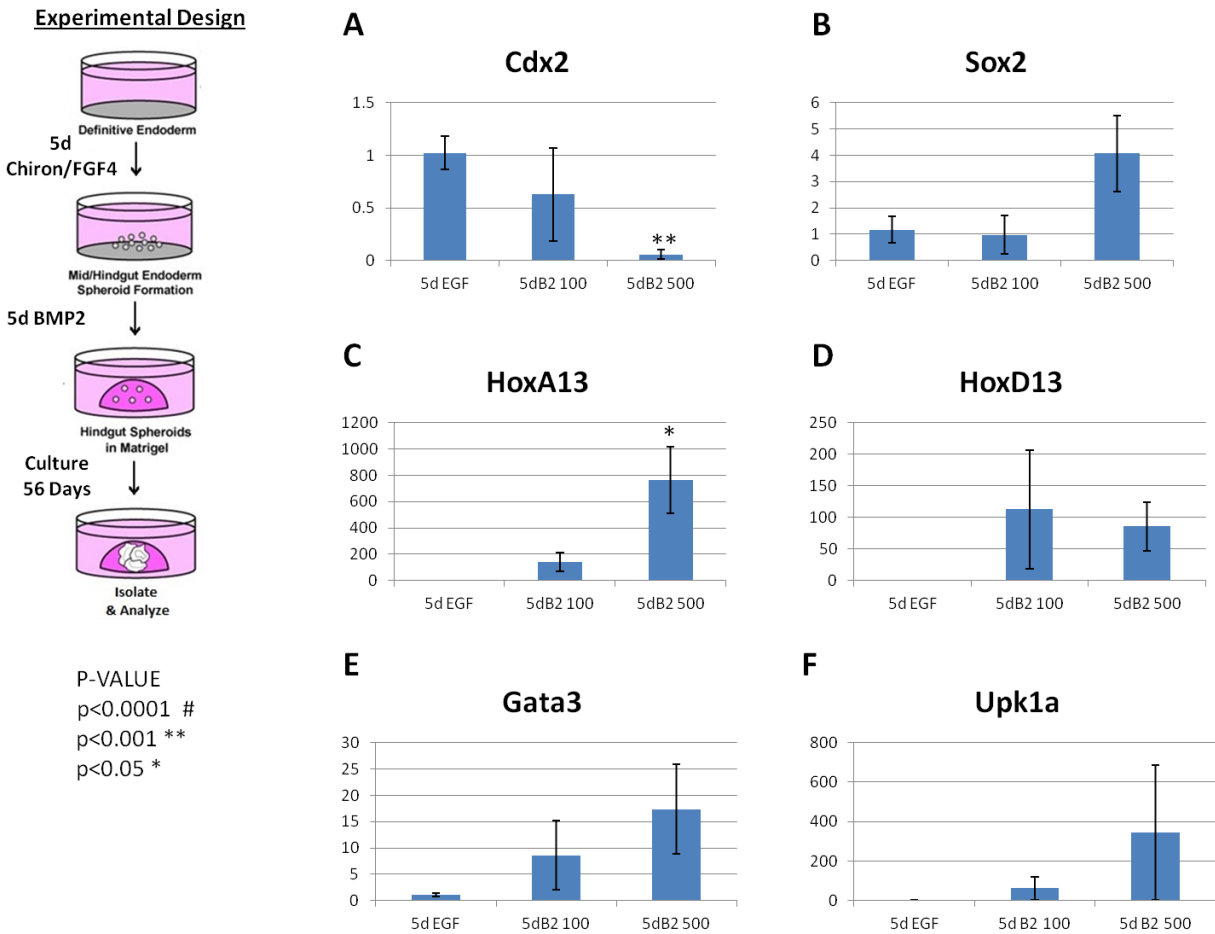


**Figure 15. Higher concentration of BMP2 results in more posterior organoids, expressing markers of urothelial differentiation**

A-F) Analysis by qPCR of 56 day organoids generated from 5 day Chiron/FGF4 treatment, 5 day BMP2 treatment at 100ng/mL or 500ng/mL. A) Relative expression of Cdx2 decreases as concentration of BMP2 increases. Decreased Cdx2 expression is statistically significantly in BMP2 at 500ng/mL organoids. B) Levels of Sox2 expression increase at 500ng/mL BMP2. C) HoxA13 expression significantly increases in BMP2 at 500ng/mL treated organoids, which is statistically significant over EGF controls, and low dose BMP2 treatment (100ng/mL). D) HoxD13 expression is increased in both BMP2 at 100ng/mL and 500ng/mL. E, F) Gata3 and Upk1a levels increase in stepwise manner with increasing concentrations of BMP2, though not statistically significant, Statistical significance was determined using unpaired, 1 tail, student t-test, where p<0.05\* and p<0.001 \*\*.

Gene	Primer-Forward	Primer-Reverse
Androgen Receptor (AR)	TTGTGTCAAAGCGAAATGG	AGTCAATGGGCAAACATGG
Beta-Tubulin	GATACCTCACCGTGGCTGCT	AGAGGAAAGGGGCAGTTGAGT
CA1	GCAAGGCTGGAGTACTTTGC	CTGGGGCAGTACAAATGAGC
Cdx2	CTGGAGCTGGAGAAGGAGTTTC	ATTTTAACCTGCCTCTCAGAGAGC
Gata3	AAAATGAACGGACAGAACCG	TTCCTCCTCCAGAGTGTGGT
HoxA13	GCACCTTGGTATAAGGCACG	CCTCTGGAAGTCCACTCTGC
HoxD13	CCTCTTCGGTAGACGCACAT	CAGGTGTAAGTGCACCAAGGA
Nkx3.1	CAGAGCCAGAGCCAGAGG	CAGATAAGACCCCAAGTGCC
Smooth muscle Actin (SMA)	CCAGAGCCATTGTCACACAC	CAGCCAAGCACTGTCAGG
Sox2	GCTTAGCCTCGTCGATGAAC	AACCCCAAGATGCACAACCTC
Upk1a	CGCACTCGAAGATGTAGACG	TAGCCAGTTTTGGTGTGGGT
Upk1b	TGGAAGCAACGAACAGTTGA	CTACCGTGTGCGCAGAAA
Upk2	ACCAGCAGGCTCTCCGTT	GATCCTGATTCTGCTGGCTC

**Table 1. qPCR primers**

List of qPCR primers, forward and reverse, for genes analyzed by qPCR.

	EGF	BMP2	BMP4	BMP7
Sox2 - 28 days	0/4	1/4	0/2	0/2
Sox2 - 56 days	0/3	0/3	1/3	0/3
Upk1a - 56 days	0/4	2/4	1/4	0/4

**Table 2. Occurrence of immune-detection of Cloacal markers, Sox2 in organoids at 28 or 56 days and Upk1a at 56 days.**

N= number of organoids with expression present/total organoids analyzed. Sox2 was identified by immunohistochemistry in one BMP2 treated organoid at 28 days, and one BMP4 organoid at 56 days. Both BMP2 and BMP4 organoids showed some expression of Upk1a at the 56 day time point.

Gene	3 FOLD increase over Average of EGF controls	Percentage of Organoids that show 3 fold or higher increase over EGF controls
<b>BMP2 Organoids</b>		
HoxA13	45/46	97.8%
HoxD13	40/46	87%
Sox2	22/47	46.8%
Upk1a	20/26	76.9%
<b>BMP4 Organoids</b>		
HoxA13	12/12	100%
HoxD13	12/12	100%
Sox2	2/12	16.7%
Upk1a	5/9	55.6%
<b>BMP7 Organoids</b>		
HoxA13	7/9	77.8%
HoxD13	4/7	57.1%
Sox2	3/9	33.3%
Upk1a	0/9	0%

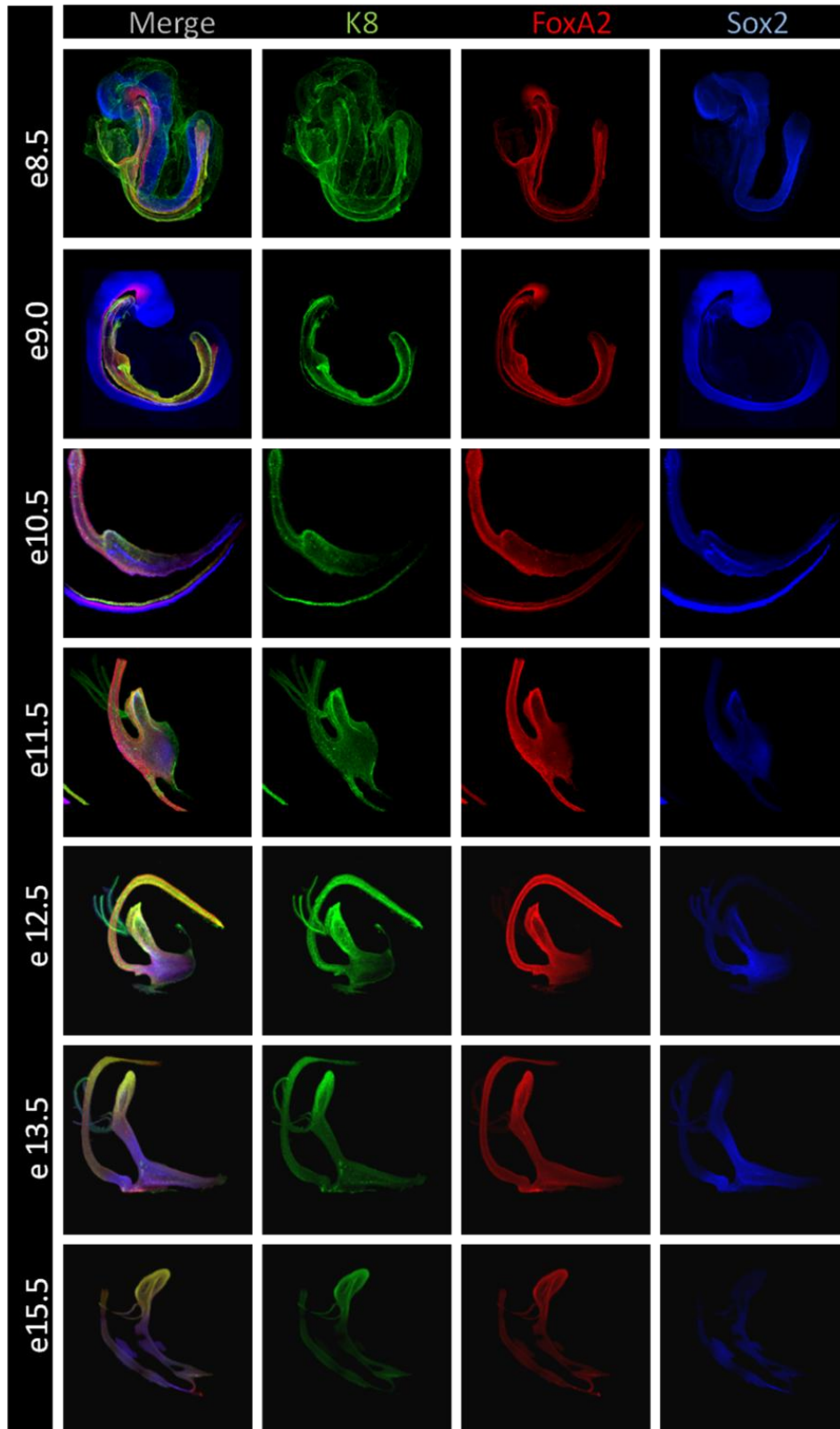
**Table 3. Incidences of 3 fold increased gene expression.**

Identified number of organoids that showed increased expression of genes (HoxA13, HoxD13, Sox2, Upk1a) at least 3 fold over average expression of EGF control organoids (average of 3 organoids when available) for BMP2, BMP4, and BMP7 treated organoids. N=number of individual organoids analyzed by qPCR. Variation in number due to differences in organoid survival and recovery. Percentages of organoids with 3 fold increased expression in far right column. BMP2 treatment shows trend in increases of HoxA13, HoxD13, Sox2, and Upk1a. BMP4 treatment shows tendency to increase HoxA13, HoxD13, and Upk1a. BMP7 shows some ability to increase HoxA13 and HoxD13. These increases are not necessarily statistically significant, rather, combines all organoids from all experimental conditions treated with indicated BMP ligand for ability to increase at least 3 fold higher gene expression than EGF control organoids.

Gene	# of Experiments where increase is statistically significant	Percentage of experiments that are statistically significant
<b>BMP2 Organoids</b>		
HoxA13	2/6	33.3%
HoxD13	2/6	33.3%
Sox2	0/13	0%
Upk1a	2/6	33.3%
<b>BMP4 Organoids</b>		
HoxA13	2/4	50%
HoxD13	3/3	100%
Sox2	0/4	0%
Upk1a	1/3	33.3%
<b>BMP7 Organoids</b>		
HoxA13	0/1	0%
HoxD13	0/1	0%
Sox2	0/3	0%
Upk1a	0/3	0%

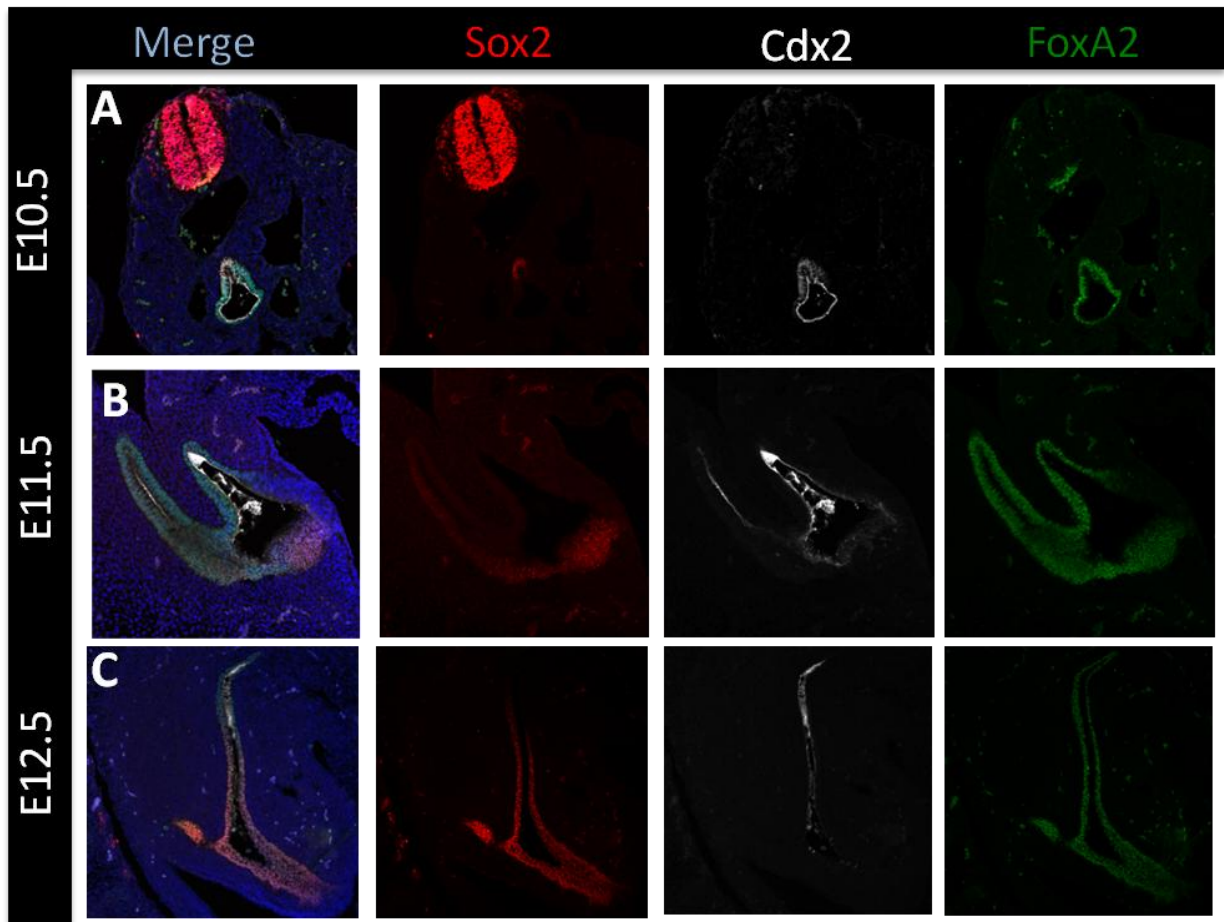
**Table 4. Number of statistically significant experiments with increased gene expression.**

Only experiments with biological triplicate were tested for statistical significance using unpaired, 1tail, student t-tests. N=number of experiments where increases in relative gene expression were statistically significant to  $p < 0.05$  for BMP ligand (2,4,7) treated organoids over EGF controls. BMP2 organoids show some statistical significance in upregulation of HoxA13, HoxD13, and Upk1a over controls. BMP4 organoids show reproducible statistically significant increases in HoxD13, and some statistical significance in HoxA13 and Upk1a over EGF controls. BMP7 organoids showed no statistically significant increases in any genes analyzed.



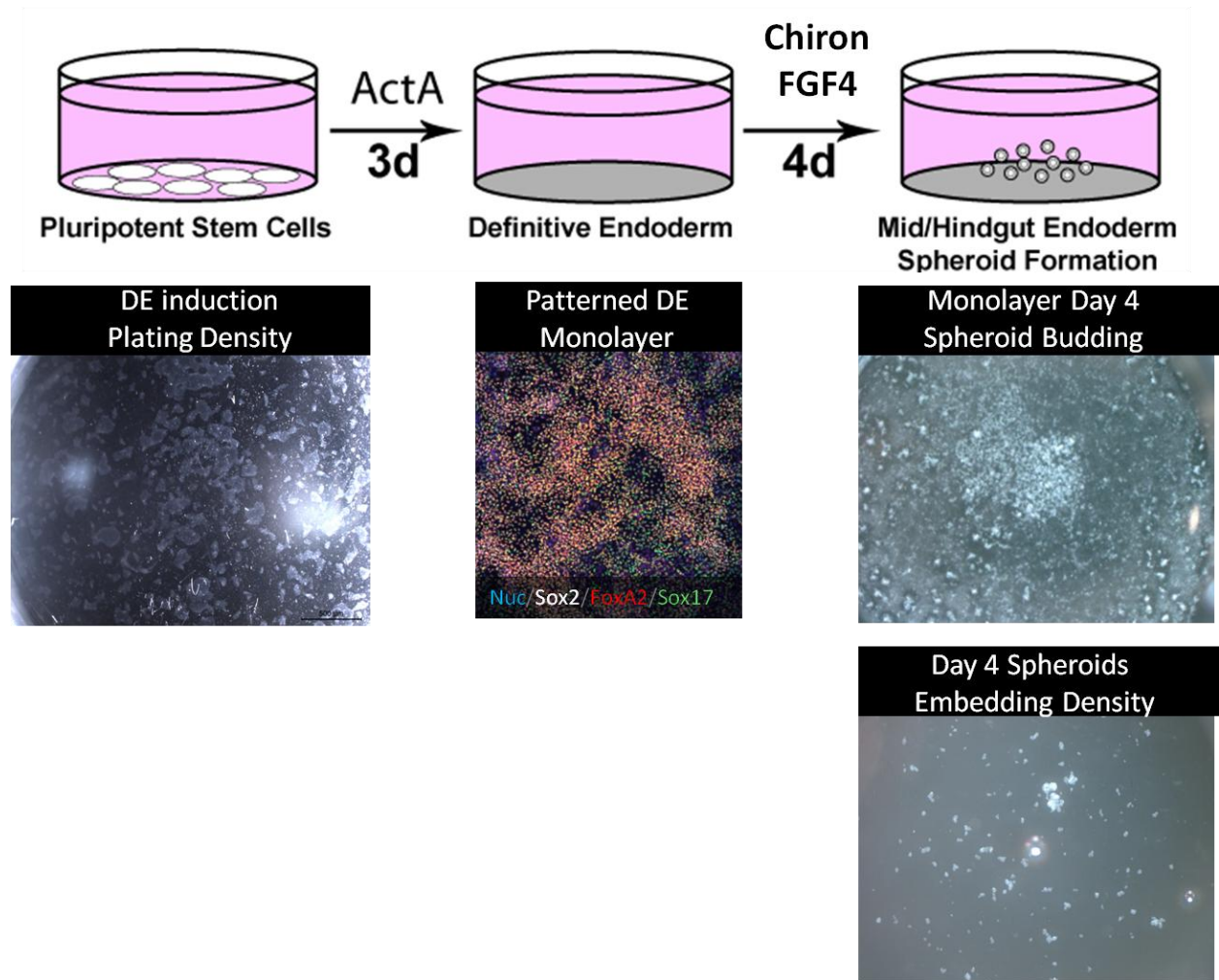
### **Supplemental Figure 1) Time course of cloacal expression of K8, Sox2, and FoxA2**

Whole mount immunostaining showing expression pattern of K8, Sox2, and FoxA2 from e8.5-e13.5 and e15.5 mouse embryos. K8 (green) expression is wide spread at e8.5 and slowly becomes restricted to the ventral anterior side of the cloacal cavity around e10.5. K8 expression continues to intensify in the budding urogenital sinus and bladder, with weaker expression observed in the anal canal and urethra e11.5-e15.5. Sox2 (Blue) is expressed in a small population of dorsal posterior hindgut cells at e8.5. Expression of Sox2 remains dorsally expressed until e11.5 when expression moves ventrally within the cloacal cavity. Sox2 becomes restricted to the anal canal and urethra from e12.5-e15.5. FoxA2 (Red) is expressed through the entire endoderm gut tube and cloaca from e8.5-e15.5. The number of embryos stained at each stage are as follows: e8.5 (n=2), e9.5 (n=3), e10.5 (n=4), e11.5 (n=4), e12.5 (n=3), e13.5 (n=2), e15.5 (n=1).



**Supplemental Figure 2) Sox2 is found in distal Cdx2 expressing cells at e10.5 during mouse embryo development.**

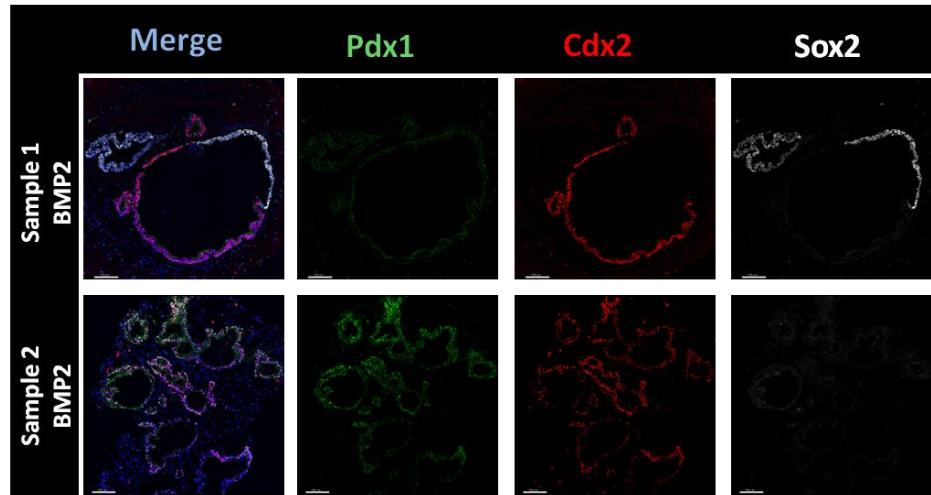
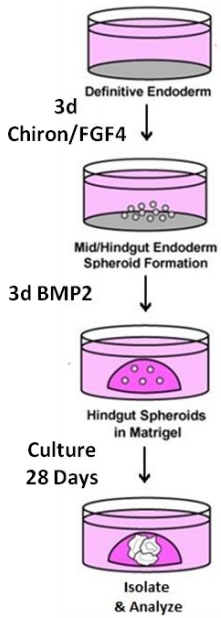
Series of paraffin sections of mouse embryos at e10.5, e11.5 and e12.5 with Immunofluorescent analysis of Sox2 (red), Cdx2 (white), FoxA2 (green) and nuclear stain dapi (blue). A) Staining at e10.5 shows small population of FoxA2 dorsal hindgut cells co-expressing Sox2 and Cdx2. B) Expression of Sox2 is restricted to the posterior dorsal region of the cloaca at e11.5 and is negative for Cdx2. C) e12.5 shows intense Sox2 staining in anal canal and cloaca/urethra but no nuclear Cdx2 expression is observed.



### Supplemental Figure 3) hESC plating and spheroid generation

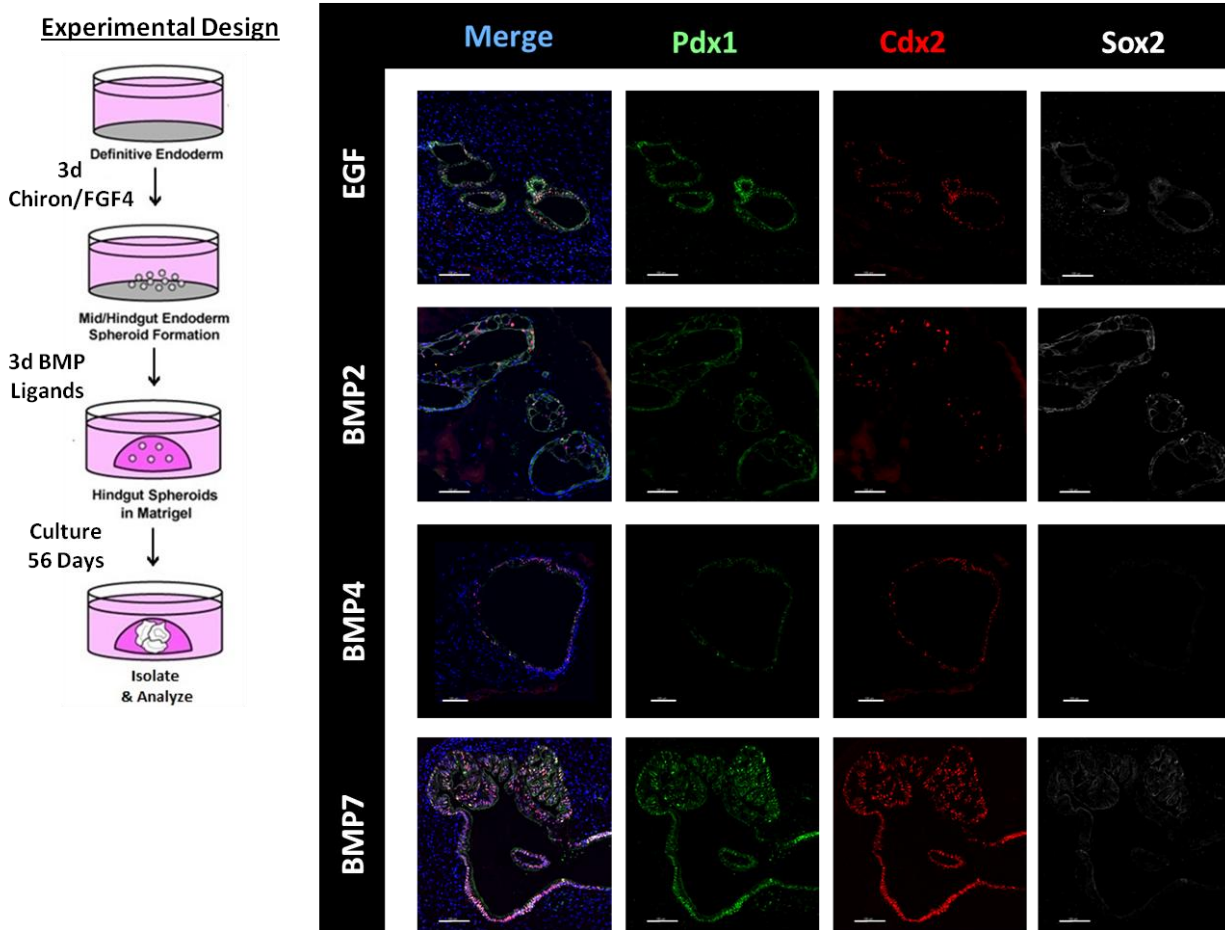
Diagram of spheroid generation. hESCs/hPSCs are plated at a density of 4 wells of a 6 well plate dispase split into a 24 well plate, as indicated by image below. After 3 days of Activin A treatment a DE monolayer is formed, that is Sox17 (green)/FoxA2 (red) double positive (approximately 85-90%), Sox2 (white) negative. Treatment of DE with Chiron/FGF4 for 4 days results in spheroids budding off the monolayer. Spheroids collect in the middle of wells (as shown) and are then embedded with approximately 50 spheroids per well (as shown).

### Experimental Design



### Supplemental Figure 4) BMP2 organoid variability at 28 days

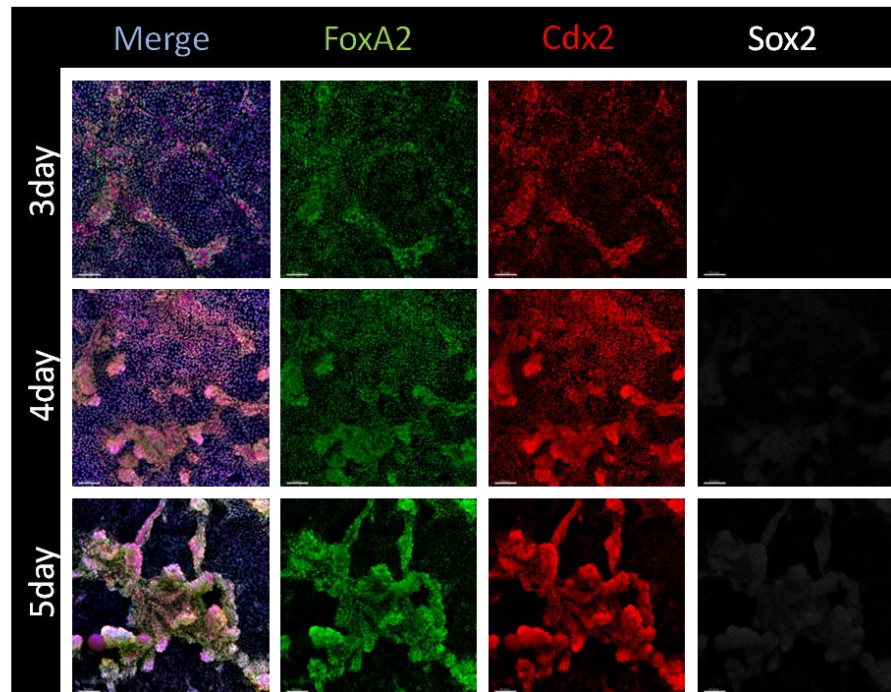
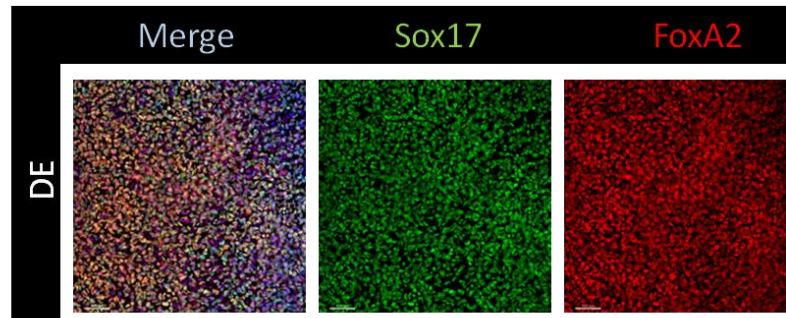
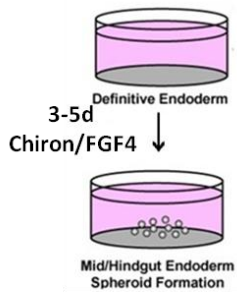
Immunofluorescent analysis at 28 days of two different BMP2 treated organoids from the same 3 day Chiron/FGF4 generated spheroids. Sample 1 (top row) shows no Pdx1 (green) staining within organoid, but strong Cdx2 (red) and Sox2 (white). Sample 2 (bottom row) shows strong Pdx1 staining that co-stains with Cdx2. Sample 2 also shows no expression of Sox2.



**Supplemental Figure 5. 56 day organoids in all conditions show expression of Pdx1**

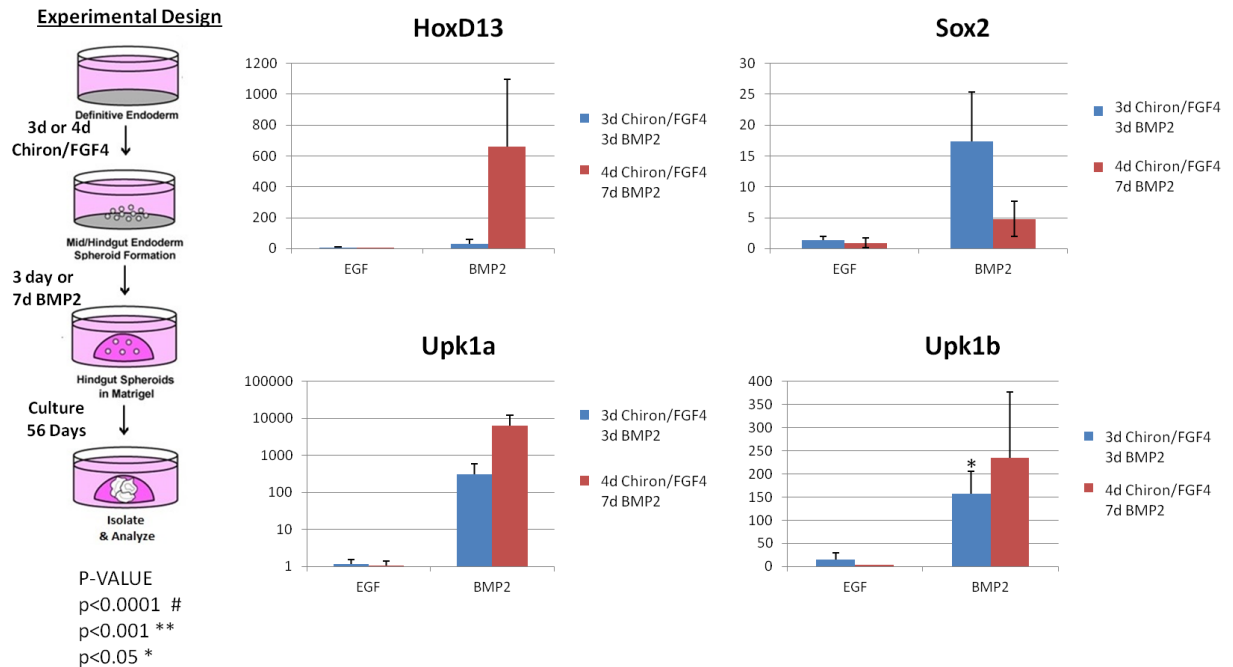
Immunofluorescent analysis at 56 days of organoids from 3 day Chiron/FGF4 spheroids treated with 3 days of BMP ligands. EGF control organoids show co-expression of Pdx1 (green), Cdx2 (red), and lack expression of Sox2 (white). BMP2, BMP4, and BMP7 treated organoids all show some degree of Pdx1 expression. BMP2 and BMP4 organoids shows some co-expression of Pdx1 with Cdx2, but lacked Sox2 expression. BMP7 organoids were almost entirely Pdx1/Cdx2 double positive and also had no expression of Sox2.

### Experimental Design



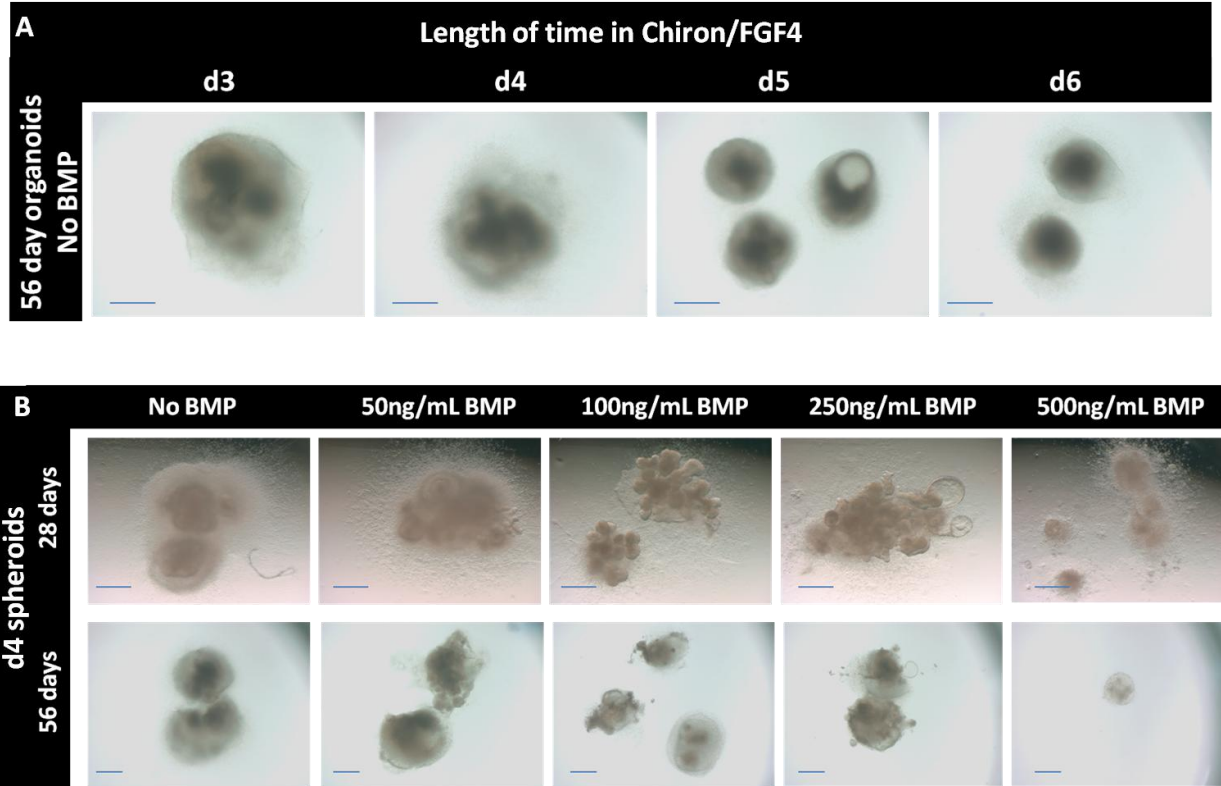
### Supplemental Figure 6. Longer Chiron/FGF4 increases three dimensional structures of monolayer

Monolayers from Chiron/FGF4 treatment after 3, 4, and 5 days were compared by immunofluorescent and morphological analysis. Top panel confirms starting DE was Sox17 (green)/FoxA2 (red) double positive. Bottom panel shows FoxA2 (green), Cdx2 (red) and Sox2 (white) on Chiron/FGF4 monolayers after 3 days, 4 days, or 5 days of treatment. All monolayers had even staining of FoxA2 and strong staining of Cdx2. Though background increased for Sox2 staining as three dimensional structures grew, no Sox2 nuclear staining was observed. Morphology of monolayers changes drastically as length in Chiron/FGF4 increases, with more Chiron/FGF4 more complex three dimensional structures form on the monolayer.



**Supplemental Figure 7. More Chiron/FGF4 and more BMP increases posterior markers and uroplakins**

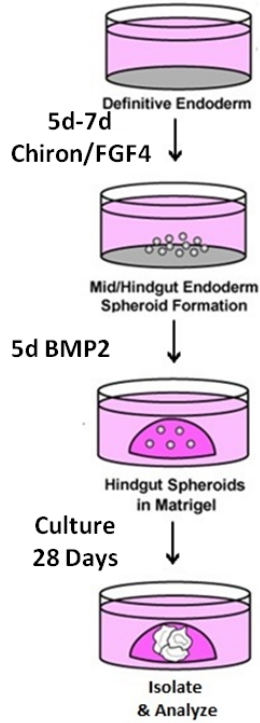
Additional analysis of organoids from Figure 13 at 56 days. Organoids from 3 day Chiron/FGF4 with 3 day BMP treatment (blue bars, data from figures 7-10) compared to organoids generated from 4 day Chiron/FGF4 with 7 days BMP2 (red bars). Increases in relative expression of HoxD13, Upk1a and Upk1b are observed in 4 day spheroids treated with 7 days of BMP2 (red bars) compared to controls, and 3 day Chiron/FGF4 treated with 3 days BMP2 (blue bars). 3 day Chiron/FGF4 with 3 days BMP2 (blue bars) showed increases in Sox2 over other conditions, and increased expression of Upk1a and Upk1b (statistically significant) over EGF controls. Statistical significance was determined using unpaired, 1 tail, student t-tests where  $p < 0.05$  \*.



**Supplemental Figure 8. More Chiron/FGF4 and higher BMP concentration causes growth retardation**

Panel A) comparison of 56 day organoids treated with only EGF from 3 days, 4 days, 5 days, or 6 days of Chiron/FGF4. Size of EGF organoids decreases as length of time in Chiron/FGF4 increases. Panel B) Comparison of organoids from 4 days of Chiron/FGF4 at 28 and 56 days that were treated with no BMP, 50ng/mL, 100ng/mL, 250ng/mL or 500ng/mL. Size of organoids at both 28 and 56 days decreases as concentration of BMP2 increases, with no BMP (EGF controls) being the largest, 50ng/mL being similar in size to the no BMP organoids, but then obvious decreases in size of BMP2 100ng/mL-500ng/mL organoids compared to controls.

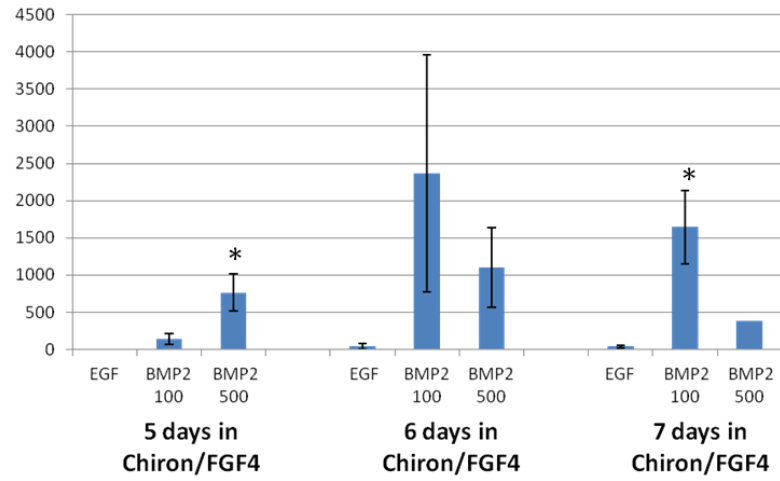
## Experimental Design



P-VALUE  
 $p < 0.0001$  #  
 $p < 0.001$  \*\*  
 $p < 0.05$  \*

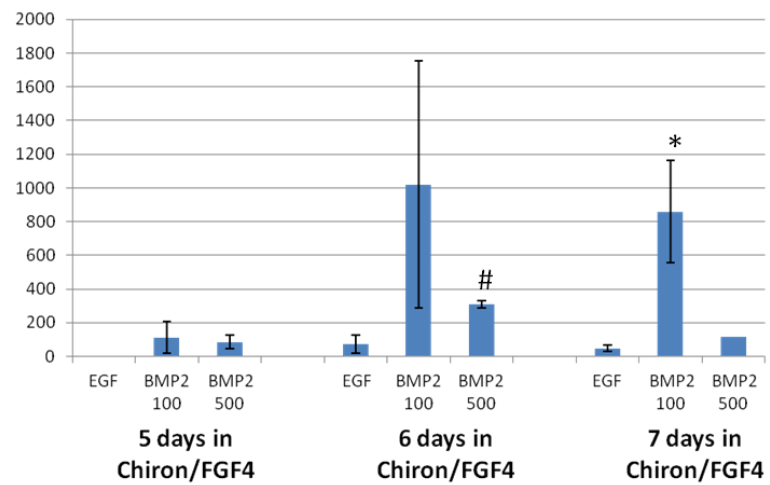
A

### HoxA13



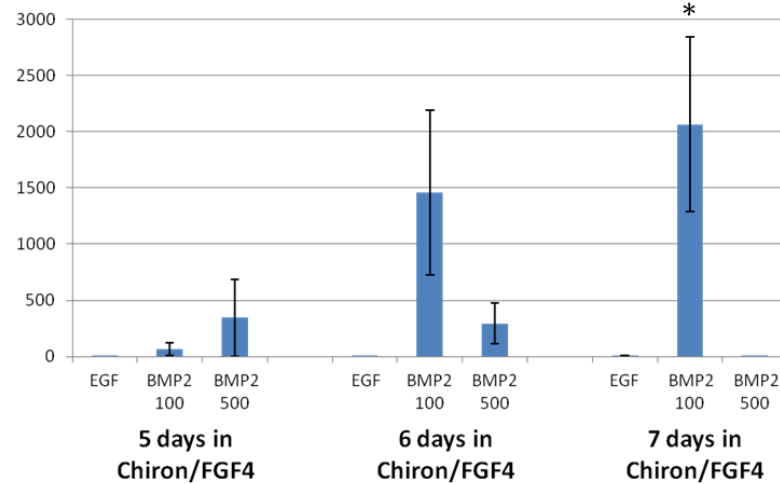
B

### HoxD13



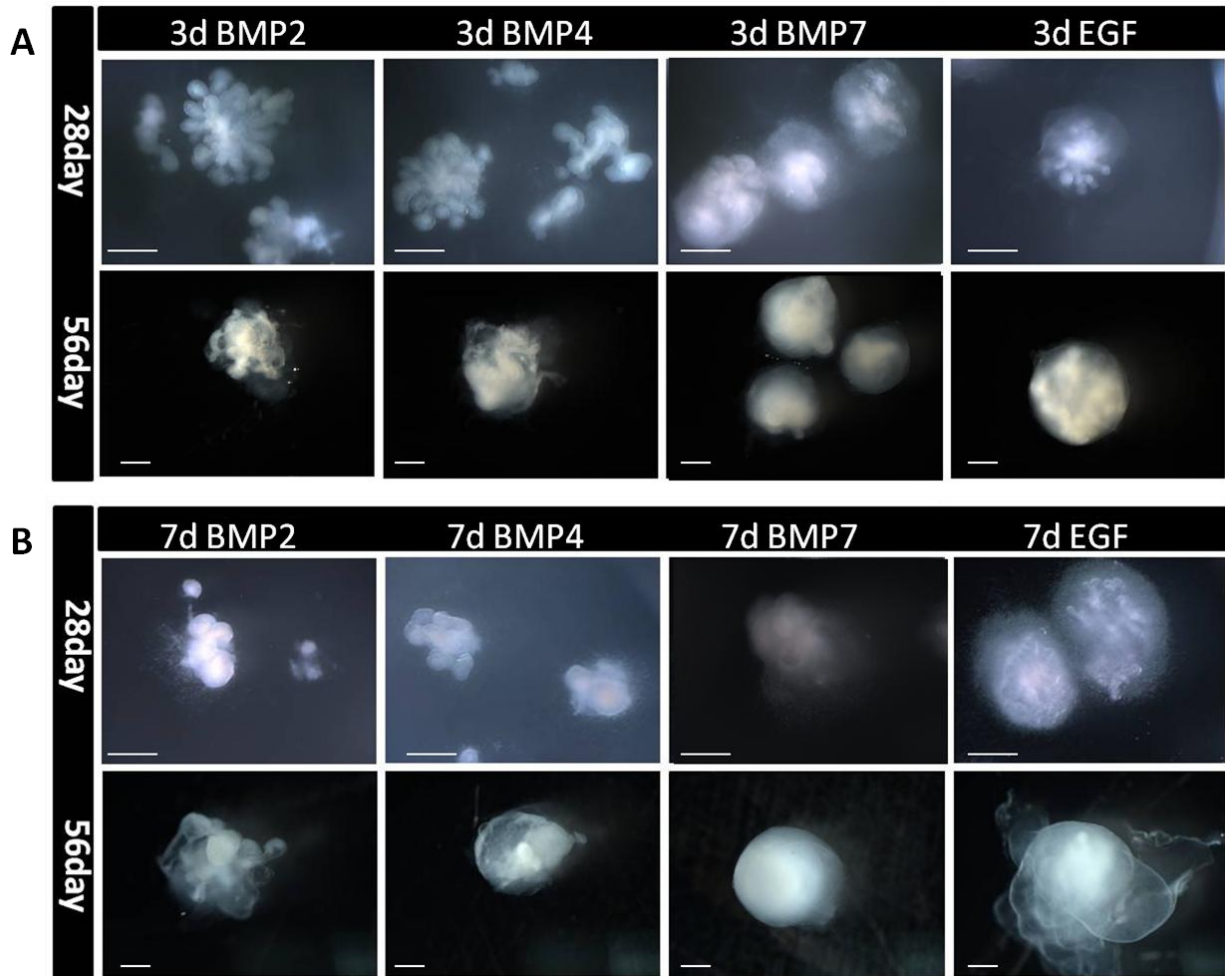
C

### Upk1a



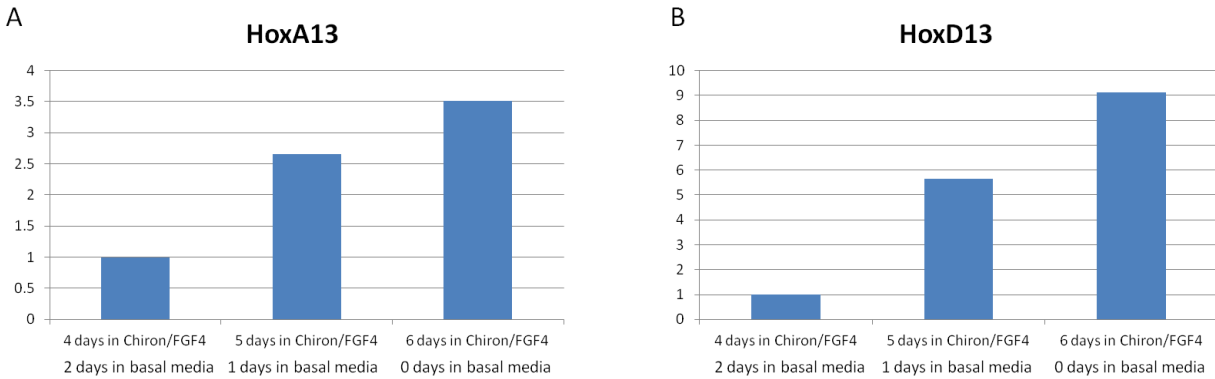
### **Supplemental Figure 9. More Chiron/FGF4 and BMP has synergistic effects on posteriorization**

Analysis by qPCR of spheroids generated from 5-7 days in Chiron/FGF4 and given no BMP (EGF control), 100ng/mL BMP2 or 500ng/mL BMP2, and cultured to 28 days. A) HoxA13 expression increases above control as concentration of BMP2 is increased though levels in 500ng/mL BMP2 are somewhat decreased in both 6 and 7 day Chiron/FGF4 spheroids. Levels also increase as days in Chiron/FGF4 increase. B) HoxD13 expression is relatively unchanged by BMP addition in 5 day Chiron/FGF4 spheroids, but is increased with the addition of 100ng/mL and 500ng/mL in 6 day spheroids, and only increased in 100ng/mL BMP2 treated 7 day spheroids. C) Upk1a expression increases in a stepwise manner in 5 day treated spheroids as BMP concentration increases. 6 day Chiron/FGF4 spheroids again show increases over control, but 100ng/mL BMP2 shows highest levels. 7 day spheroids show the highest relative levels of Upk1a when treated with BMP2 at 100ng/mL. Statistical significance was determined using unpaired, 1 tail, student t-tests (5 day Chiron/FGF4 spheroids treated with EGF were used as controls for all comparisons) where  $p < 0.05$  \*,  $p < 0.0001$  #.



### Supplemental Figure 10. Morphological differences between BMP ligands

Morphological comparison of organoids from 3 day Chiron/FGF4 with 3 day BMP treatment (panel A) compared to organoids generated from 4 day Chiron/FGF4 with 7 days BMP (panel B). A) Morphology of organoids varies significantly. BMP7 treated organoids show an increase in mesenchyme and less complex epithelial structure. BMP2 and BMP4 organoids share similar morphology at both 28 and 56 days in culture, with multiple budding branches. EGF organoids have more mesenchyme than BMP2/4 organoids, but less than BMP7, surrounding an epithelial structure. B) Organoids from 4 day Chiron/FGF4 and longer BMP treatment are smaller and show less complexity than those in panel A. BMP2 and BMP4 organoids are similar in size and structure, with few buds. BMP7 organoids are less complex and contain the most mesenchyme. EGF organoids show complex epithelial structure, with branching surrounded by a thick layer of mesenchyme.



**Supplemental Figure 11. Extended Chiron/FGF4 causes spheroid age independent posteriorization**

Comparison of posterior hox gene expression in spheroids that were harvest after 4, 5, or 6 days in Chiron/FGF4 that were age matched. Spheroids from 4 days of Chiron/FGF4 were aged for 2 days floating in low attachment dish with media containing no growth factors. Spheroids from 5 days of Chiron/FGF4 were aged 1 day floating in low attachment dish with no growth factors supplementing media. All spheroids were collected on same day to ensure similar age. Analysis by qPCR for posterior Hox genes (A-B) show age matched spheroids show increase in relative expression levels of HoxA13 (A) and HoxD13 (B) as they are exposed to longer periods of Chiron/FGF4. Statistical significance is not calculated, as one sample (75-100 spheroids total) was analyzed per condition.

## References

Beltrão-Braga PC, et al. In-a-dish: Induced pluripotent stem cells as a novel model for human diseases. 2013;83(1):11-7. [PubMed: 23281003]

Chia I, et al. Nephric duct insertion is a crucial step in urinary tract maturation that is regulated by a Gata-3-Raldh2-Ret molecular network in mice. *Development*. 2011; 138(10):2098-2097. [PubMed: 21521737]

Cunha GR, et al. Hormonal, cellular, and molecular regulation of normal and neoplastic prostatic development. *J Steroid Biochem Mol Bio*. 2004; 92(4):221-36.[PubMed: 15663986]

D'Amour KA, et al. Efficient differentiation of human embryonic stem cells to definitive endoderm. *Nat Biotechnol*. 2005;23:1534-1541. [PubMed: 16258519]

Dessimoz J, Opoka R, Kordich JJ, Grapin-Botton A, Wells JM. FGF signaling is necessary for establishing gut tube domains along the anterior-posterior axis in vivo. *Mech Dev*. 2006; 123:42-55. [PubMed:16326079]

Eom D, et al. Bone Morphogenetic proteins regulate neural tube closure by interacting with the apicobasal polarity pathway. *Development*. 2011;138(15):3179-3188. [PubMed:21750029]

Fairbanks TJ, et al. Fibroblast growth factor 10 (Fgf10) invalidation results in anorectal malformation in mice. *J Pediatr Surg*. 2004;39(3):360-5. [PubMed: 15017552]

Gros J, et al. Wnt5a/JNK and FGF/MAPK pathways regulate the cellular events shaping the vertebrate limb bud. *Curr Biol*. 2010;20(22):1993-2002 [PubMed: 21055947]

Islam SS, et al. Spatio-temporal distribution of Smads and role of Smads/TGF- $\beta$ /BMP-4 in the regulation of mouse bladder organogenesis. *PLoS One*. 2013;8(4):e61340. [PubMed: 23620745]

Itzhaki I, et al. Modelling the long QT syndrome with induced pluripotent stem cells. Nature. 2011;471(7337):225-9. [PubMed: 21240260]

Jia H, et al. Wnt5a expression in the hindgut of fetal rats with chemically induced anorectal malformations—studies in the ETU rat model. *Int J Colorectal Dis*. 2011;24(4):493-9. [PubMed: 21212964]

- Kimmel SG, et al. New mouse models of congenital anorectal malformations. *J Pediatr Surg.* 2000;35(2):227-30. [PubMed: 10693670]
- Kluth, D. Embryology of anorectal malformations. *Semin Pediatr Surg.* 2010;19(3): 201-108.[PubMed: 20610193]
- Kroon E, et al. Pancreatic endoderm derived from human embryonic stem cells generates glucose-responsive insulin-secreting cells in vivo. *Nat Biotechnol.* 2008;26(4):443-52.[PubMed:18288110]
- Kumar M, et al. Signals from lateral plate mesoderm instruct endoderm toward a pancreatic fate. *Dev Biol.* 2003;259(1):109-22. [PubMed: 12812792]
- Levitt MA, Pena A. Cloacal malformations: lessons learned from 490 cases. *Semin Pediatr Surg.* 2010;19:128-138. [PubMed: 20307849]
- Levitt MA, Pena A. Anorectal malformations. *Orphanet J Rare Dis.* 2007;2:33. [PubMed 17651510]
- Li FF, et al. Spatiotemporal expression of Wnt5a during the development of the hindgut and anorectum in human embryos. *Int J Colorectal Dis.* 2011;26(8):983-8. [PubMed: 21431850]
- McCracken KW, et al. Generating human intestinal tissue from pluripotent stem cells in vitro. *Nat. Protoc.* 2011;6(12):1920-8. [PubMed: 22082986]
- McLin VA, Rankin SA, Zorn AM. Repression of Wnt/Beta-Catenin signaling in the anterior endoderm is essential for liver and pancreas development. *Development.* 2007; 134:2207-2217. [PubMed: 17507400]
- Mo R, et al. Anorectal malformations caused by defects in sonic hedgehog signaling. *Am J Pathol.* 2001;159:765-774 [PubMed: 1850556]
- Mortlock DP, Innis JW. Mutation of HOXA13 in hand-foot-genital syndrome. *Nat Genet.* 1997;15(2):179-80. [PubMed: 9020844]
- Mueller TD, et al. Promiscuity and specificity in BMP receptor activation. *FEBS Lett.* 2012; 586(14):1846-59. [PubMed:22710174]
- Penington EC, et al. The cloacal plate: the missing link in anorectal and urogenital development. *BJU int.* 2002; 89(7):726-732. [PubMed: 11966633]
- Pyati UJ, et al. Sustained Bmp signaling is essential for cloaca development in zebrafish. *Development.* 2006; 133(11):2275-2284. [PubMed:16672335]

Ramel MC, et al. Spatial regulation of BMP activity. *FEBS Lett.* 2012; 586(14):1929-41. [PubMed: 22710177]

Rankin SA, et al. A gene regulatory network controlling *hhx* transcription in the anterior endoderm of the organoizer. *Dev Biol.* 2011;351(2):297-310. [PubMed: 21215263]

Runck et al. Defining The Molecular Pathologies in Cloaca Malformation: Similarities Between Mouse and Human. *Disease Models Mech.* 2013. Sumbitted.

Sasaki Y, et al. Sonic hedgehog and bone morphogenetic protein 4 expressions in the hindgut region of murine embryos with anorectal malformations. *J Pediatr Surg.* 2004;39(2):170-3. [PubMed: 14966734]

Seifert AW, et al. Cell lineage analysis demonstrates an endodermal origin of the distal urethra and perineum. *Dev Biol.* 2008;318(1):143-52. [PubMed: 18439576]

Seifert AW, et al. Sonic hedgehog controls growth of external genitalia by regulating cell cycle kinetics. *Nature communications.* 2010; 1:23. [PubMed: 20975695]

Seifert AW, et al. Multiphasic and tissue-specific roles of sonic hedgehog in cloacal septation and external genitalia development. *Development.* 2009;136:394903957. [PubMed: 19906862]

Shah D, et al. Bilateral microphthalmia, esophageal atresia, and cryptorchidism: the anophthalmia-esophageal-genital syndrome. *Am J Med Genet.* 1997;70(2):171-3. [PubMed: 9128938]

Silberg DG, et al. *Cdx1* and *Cdx2* expression during intestinal development. *Gastroenterology.* 2000; 119(4):961-71. [PubMed: 11040183]

Spence JR, et al. Directed differentiation of human pluripotent stem cells into intestinal tissue in vitro. *Nature.* 2011; 470:105-109. [PubMed: 21151107]

Tai CC, et al. *Wnt5a* Knock-out mouse as a new model of anorectal malformation. *J Surg Res.* 2009;156(2):278-82. [PubMed:19577771]

Tucker JA, et al. The BMP signaling gradient patterns dorsoventral tissues in a temporally progressive manner along the anteroposterior axis. *Dev Cell.* 2008;14(1):108-19. [PubMed: 18194657]

Warne SA, et al. Understanding cloacal anomalie. *Arch Dis Child.* 2011; 96(11):1072-6. [PubMed: 21262748]

Wang C, et al. Embryonic origin and remodeling of the urinary and digestive outlets. *PLoS One.*2013; 8(2):e55587. [PubMed: 23390542]

Wang C, et al. Six1 and Eya1 are critical regulators of peri-cloacal mesenchymal progenitors during genitourinary tract development. *Dev Biol.* 2011; 360(1):186-94. [PubMed: 21968101]

Wang S, et al. Human iPSC-derived oligodendrocyte progenitor cells can myelinate and rescue a mouse model of congenital hypomyelination. *Cell Stem Cell.* 2013; 12(2):252-64. [PubMed: 23395447]

Wells JM, Melton DA. Early mouse endoderm is patterned by soluble factors from adjacent germ layers. *Development.* 2000; 127:1563-1572. [PubMed: 10725233]

Williamson KA, et al. Mutations in SOX2 cause anophthalmia-esophageal-genital (AEG) syndrome. *Hum Mol Genet.* 2006;15(9):1413-22. [PubMed: 16543359]

Wu X, et al. Bmp7 expression and null phenotype in the urogenital system suggest a role in re-organization of the urethral epithelium. *Gene Expr Patterns.* 2009; 9(4):224-30. [PubMed: 19159697]

Xu K, et al. Bmp7 functions via a polarity mechanism to promote cloacal septation. *PLoS One.* 2012;7(1):e29372. [PubMed: 22253716]

Zhang J, et al. Down-regulation of SHH/BMP4 signaling in human anorectal malformations. *J Int Med Res.* 2009; 37(6):1842-50. [PubMed: 20146882]

Zorn AM, Wells JM. Molecular basis of vertebrate endoderm development. *Int Rev Cytol.* 2007;259:49-111. [PubMed:17425939]